

Figure 4. Dose-dependent induction for mRNA of metabolic enzymes measured by RT-PCR in HepG2 cells exposed to PAHs and oxy-PAHs for 24 h. (A) P4501A1 mRNA, (B) P4501A2 mRNA, (C) NQO1 mRNA, and (D) GSTM1 mRNA were measured.

Table 1. P4501A1 mRNA Induction in HepG2 Cells (for 24 h) by PAHs, oxy-PAHs, and TCDD

compound	EC <sub>TCDD25</sub> (nM) <sup>a</sup>	IEF <sup>b</sup>
B[a]P	$1.3 \times 10^3$	1
B[k]FA	13	100
DB[a,h]A	200	6.7
IdP	350	3.8
NCQ	$2.0 \times 10^3$	0.66
B[b]FO	$2.3 \times 10^3$	0.58
TCDD	0.068	$1.9 \times 10^4$

<sup>a</sup> Concentration equivalent with 25% of TCDD max (P4501A1 mRNA induction). <sup>b</sup> IEF relative to B[a]P (P4501A1 mRNA induction).

uted to the strong AhR-mediated induction of P4501A1 mRNA even after 72 h (12). It was shown that many DNA adducts caused by oxygenated metabolites such as hydroxyepoxides and bisdiols were formed when animals or culture cells were exposed to IdP and DB[a,h]A (43, 44). Indeed, high levels of formation of oxygenated metabolites may explain the strong P4501A1 mRNA induction for IdP and DB[a,h]A even after 72 h. In the case of oxy-PAHs NCQ and B[b]FO, continual P4501A1 mRNA induction, even after 72 h, may have been generated by oxygenated metabolites or ROS formation. The study for examining these possibilities is underway.

Penning et al. reported that the induction of AKR1C1 mostly occurred in four human isoforms of AKRs (AKR1C1–AKR1C4) when HepG2 cells and human colon carcinoma (HT29) cells were exposed to antioxidants such as  $\beta$ -NF and *tert*-butylhydroquinone and ROS such as H<sub>2</sub>O<sub>2</sub> (13). They reported also that *trans*-dihydrodiols of some PAHs (naphthalene, phenanthrene, B[a]A, Chr, B[a]P, etc.) were converted to PAH catechols by several AKRs (21). In our study, the mRNA induction levels of AKR1C1 were significantly high at the exposure to 5  $\mu$ M oxy-PAHs such as NCQ, B[a]FO, B[b]FO, CPPO, and  $\beta$ -NF (Figure 3A). The rapid increase for the

induction of AKR1C1 mRNA via activated AP-1 was observed for oxy-PAHs NCQ and B[b]FO (Figure 5B); therefore, it is possible that these compounds themselves are AP-1 active compounds and AKR1C1 inducers. P450s-inducing PAHs such as B[a]P, B[k]FA, and DB[a,h]A at 5  $\mu$ M also induced AKR1C1 mRNA significantly for 24 h, and the start of AKR1C1 mRNA inductions for B[a]P, B[k]FA, and DB[a,h]A required more than 6 h. Therefore, it is suggested that some P4501A1-catalyzed electrophilic oxygenated metabolites of PAHs (Michael reaction acceptors) or ROS generated from these metabolites contributed to the induction of AKR1C1 mRNA (Figures 2, 3A, and 5B).

Cytosolic NQO1 is the enzyme that catalyzes two-electron reduction and detoxification of quinones, repressing one-electron reduction of quinones by microsomal NADPH-dependent cytochrome P450 reductase and mitochondrial NADH-dependent ubiquinone oxidoreductase (9, 15–17, 21, 28, 29, 45). Several PAH quinones were reduced via both one- and two-electron reductions (21, 29). In our study, the mRNA induction levels of NQO1 were high after PAH exposure for 24 h at 5  $\mu$ M except for TPh and B[ghi]Pe and this pattern is similar to P4501A1 and 1A2. However, the point that oxy-PAHs such as BAQ, NCQ, B[a]FO, B[b]FO, and  $\beta$ -NF at 5  $\mu$ M induced NQO1 mRNA at the same levels as these nonoxy-PAHs was different from the patterns of P4501A1 and 1A2 mRNA induction. The tendency for a rapid increase in NQO1 mRNA induction from 6 h for most PAHs and oxy-PAHs is similar to AKR1C1 and the slightly higher rate increase of NQO1 mRNA induction for oxy-PAHs, NCQ, and B[b]FO, more than for nonoxy-PAHs, is also similar to AKR1C1 (Figure 5C). That the induction of NQO1 mRNA did not decrease from 24 to 72 h for B[k]FA, DB[a,h]A, and IdP is similar to P4501A1. NQO1 is regulated by both XRE (AhR) and EpRE (AP-1), so the result of the induction of NQO1 mRNA is thought to be the mixed type of

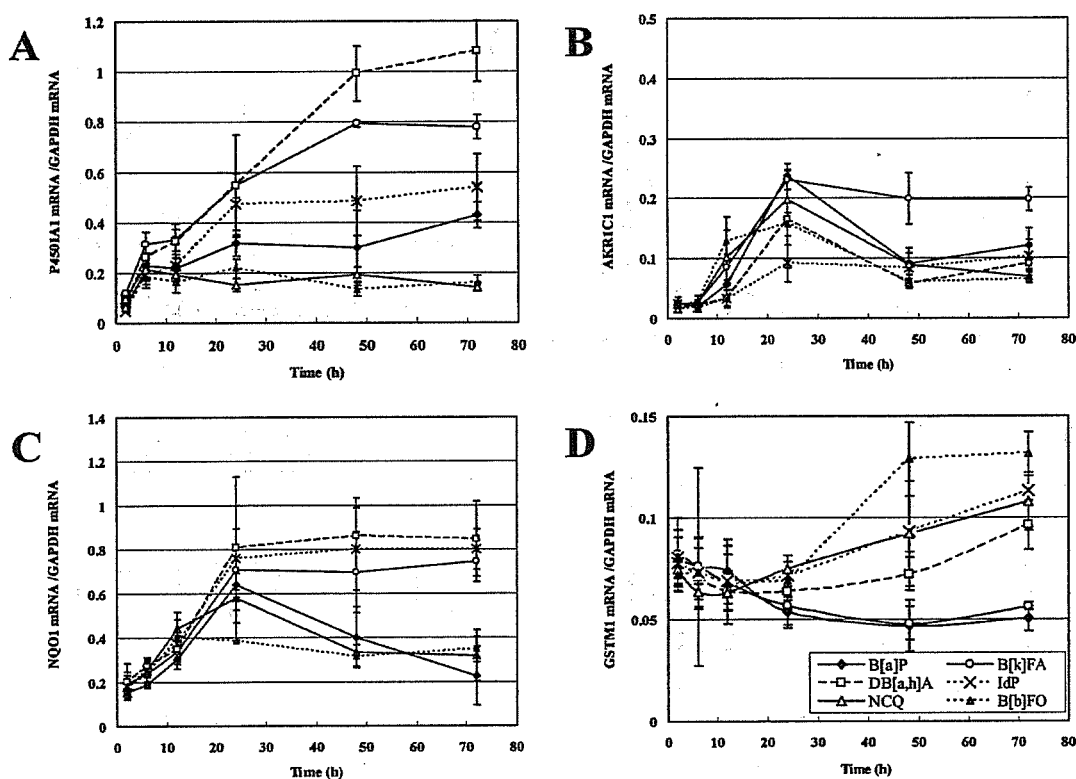


**Figure 5.** Time-dependent induction for mRNA of metabolic enzymes measured by RT-PCR in HepG2 cells exposed to 5  $\mu$ M PAHs and oxy-PAHs. (A) P4501A1 mRNA, (B) AKR1C1 mRNA, (C) NQO1 mRNA, and (D) GSTM1 mRNA were measured.

P4501A1 mRNA and AKR1C1 mRNA based upon chemical dependency and time-dependent curves (Figures 2, 3, and 5). The contribution to NQO1 mRNA induction via EpRE (electrophiles or ROS) may be more than the contribution by AhR because the promoter of the human *NQO1* gene contains an imperfect XRE (17).

GSTAs, GSTMs, GSTPs, and GSTTs are included in human isoenzymes of GST (17, 46, 47). These GSTs catalyze GSH conjugation with ROS or B[a]P metabolites such as epoxides (BPDE, etc.) and quinones (BPQ, etc.) (12, 17, 21, 48). In HepG2 cells exposed to a Me<sub>2</sub>SO control and some PAHs and oxy-PAHs, the mRNA levels of GSTA1 and GSTP1 were at least two magnitudes lower than GSTM1 in additional RT-PCR (data not shown); so, in this study, the GSTM1 isoform was measured in detail (42, 47). The frequency of deficiency of the *GSTM1* gene is higher than other *GST* genes in humans (14, 17), and the promoter of the *GSTM1* gene also contains both XRE and EpRE (17); however, in this study, mRNA induction was not dramatically increased by any PAH and oxy-PAH. Although the tendency for decrease in GSTM1 mRNA in the dose-response curves for several PAHs and oxy-PAHs and in the time-course curve for all PAHs and oxy-PAHs was observed and these decreases were much greater for B[a]P and B[k]FA, the mechanism of these phenomena was not clear (Figures 4D and 5D). It may be derived from a shortage of GSH during reactions with ROS or diolepoxides (49).

In conclusion, the pattern for induction of metabolic enzymes by three nonoxy-PAHs (B[k]FA, DB[a,h]A, and IdP) was similar to B[a]P. Considering this, mechanisms of metabolism by them are possibly similar to B[a]P. In the case of oxy-PAHs, the general mechanisms of induction of metabolic enzymes may be similar to that of quinone-yielding ROS (21, 45). It will be necessary to examine the relationships between metabolite

formation of PAHs and oxy-PAHs and DNA adduct formation and metabolic enzyme induction by them in detail. Additionally, it will be interesting to examine the patterns of metabolic enzyme induction and DNA adduct formation after compound exposure by using target organ cells in carcinogenesis studies in the future.

**Acknowledgment.** We thank Robert Kanaly, Department of Environmental Biosciences and International Graduate School of Arts and Sciences, Yokohama City University, Yokohama, Japan, for help in manuscript preparation. This work was supported in part from the Ministry of Health, Labour and Welfare and Grants-in-Aid for Scientific Research on Priority Areas (13027245, 16201012, and 18101003) from the Japanese Ministry of Education, Science, Sports and Culture.

## References

- (1) Hannigan, M. P., Cass, G. R., Penman, B. W., Crespi, C. L., Lafleur, A. L., Busby, W. F., Jr., Thilly, W. G., and Simoneit, B. R. T. (1998) Bioassay-directed chemical analysis of Los Angeles airborne particulate matter using a human cell mutagenicity assay. *Environ. Sci. Technol.* 32, 3502-3514.
- (2) Rogge, W. F., Hildemann, L. M., Mazurek, M. A., and Cass, G. R. (1993) Sources of fine organic aerosol. 2. Noncatalyst and catalyst-equipped automobiles and heavy-duty diesel trucks. *Environ. Sci. Technol.* 27, 636-651.
- (3) Alskog, T., Strandell, M., Westerholm, R., and Stenberg, U. (1985) Fractionation and chemical analysis of gasoline exhaust particulate extracts in connection with biological testing. *Environ. Int.* 11, 249-257.
- (4) Fernandez, P., and Bayona, J. M. (1992) Use of off-line gel permeation chromatography-normal-phase liquid chromatography for the determination of polycyclic aromatic compounds in environmental samples and standard reference materials (air particulate matter and marine sediment). *J. Chromatogr.* 625, 141-149.
- (5) IARC. (1983) Polynuclear aromatic compounds, Part 1, Chemical, environmental and experimental data. *IARC Monographs on the Evaluation of the Carcinogenic Risk of Chemicals to Humans*, Vol. 32, IARC, Lyon, France.

- (6) Monarca, S., Feretti, D., Zanardini, A., Moretti, M., Villarini, M., Spiegelhalter, B., Zerbini, I., Gelatti, U., and Lebbolo, E. (2001) Monitoring airborne genotoxicants in the rubber industry using genotoxicity tests and chemical analysis. *Mutat. Res.* 490, 159–169.
- (7) Straif, K., Baan, R., Grosse, Y., Secretan, B., Ghissassi, F. E., and Coglianò, V. (2005) Carcinogenicity of polycyclic aromatic hydrocarbons. *Lancet Oncol.* 6, 931–932.
- (8) Durant, J. L., Busby, W. F., Jr., Lafleur, A. L., Penman, B. W., and Crespi, C. L. (1996) Human cell mutagenicity of oxygenated, nitrated and unsubstituted polycyclic aromatic hydrocarbons associated with urban aerosols. *Mutat. Res.* 371, 123–157.
- (9) Pelkonen, O., and Nebert, D. W. (1982) Metabolism of polycyclic aromatic hydrocarbons: Etiologic role in carcinogenesis. *Pharmacol. Rev.* 34, 189–222.
- (10) Møller, M., Hagen, I., and Ramdahl, T. (1985) Mutagenicity of polycyclic aromatic compounds (PAC) identified in source emissions and ambient air. *Mutat. Res.* 157, 149–156.
- (11) Tada, K., Odashima, N., and Ishidate, M. (1966) On the screening experiment for the carcinogenicity of polycyclic quinones. *Kyoritsu Pharm. Univ. Environ. Doc.* 63–68.
- (12) Burczynski, M. E., and Penning, T. M. (2000) Genotoxic polycyclic aromatic hydrocarbon *ortho*-quinones generated by aldo-keto reductases induce CYP1A1 via nuclear translocation of the aryl hydrocarbon receptor. *Cancer Res.* 60, 908–915.
- (13) Burczynski, M. E., Lin, H.-S., and Penning, T. M. (1999) Isoform-specific induction of a human aldo-keto reductase by polycyclic aromatic hydrocarbons (PAHs), electrophiles, and oxidative stress: Implications for the alternative pathway of PAH activation catalyzed by human dihydrodiol dehydrogenase. *Cancer Res.* 59, 607–614.
- (14) Sachse, C., Smith, G., Wilkie, M. J. V., Barrett, J. H., Waxman, R., Sullivan, F., Forman, D., Bishop, D. T., Wolf, C. R., and the Colorectal Cancer Study Group (2002) A pharmacogenetic study to investigate the role of dietary carcinogens in the etiology of colorectal cancer. *Carcinogenesis* 23, 1839–1849.
- (15) Talalay, P. (1989) Mechanisms of induction of enzymes that protect against chemical carcinogenesis. *Adv. Enzyme Regul.* 28, 237–250.
- (16) Prester, T., Holtzclaw, W. D., Zhang, Y., and Talalay, P. (1993) Chemical and molecular regulation of enzymes that detoxify carcinogens. *Proc. Natl. Acad. Sci. U.S.A.* 90, 2965–2969.
- (17) Hayes, J. D., and Pulford, D. J. (1995) The glutathione S-transferase supergene family: Regulation of GST\* and the contribution of the isoenzymes to cancer chemoprotection and drug resistance. *Crit. Rev. Biochem. Mol. Biol.* 30, 445–600.
- (18) Cavaieri, E. L., and Rogan, E. G. (1995) Central role of radical cations in metabolic activation of polycyclic aromatic hydrocarbons. *Xenobiotica* 25, 677–688.
- (19) Melendez-Colon, V. J., Luch, A., Seidel, A., and Baird, W. M. (1999) Cancer initiation by polycyclic aromatic hydrocarbons results from formation of stable DNA adducts rather than apurinic sites. *Carcinogenesis* 20, 1885–1891.
- (20) Park, J.-H., Troxel, A. B., Harvey, R. G., and Penning, T. M. (2006) Polycyclic aromatic hydrocarbon (PAH) *o*-quinones produced by the aldo-keto-reductases (AKRs) generate abasic sites, oxidized pyrimidines, and 8-oxo-dGuo via reactive oxygen species. *Chem. Res. Toxicol.* 19, 719–728.
- (21) Bolton, J. L., Trush, M. A., Penning, T. M., Dryhurst, G., and Monks, T. J. (2000) Role of quinones in toxicology. *Chem. Res. Toxicol.* 13, 135–160.
- (22) Kim, K. B., and Lee, B. M. (1997) Oxidative stress to DNA, protein, and antioxidant enzymes (superoxide dismutase and catalase) in rats treated with benzo(a)pyrene. *Cancer Lett.* 113, 205–212.
- (23) Canova, S., Degan, P., Peters, L. D., Livingstone, D. R., Voltan, R., and Venier, P. (1998) Tissue dose, DNA adduct, oxidative DNA damage and CYP1A-immunopositive proteins in mussels exposed to waterborne benzo(a)pyrene. *Mutat. Res.* 399, 17–30.
- (24) Leadon, S. A. (1987) Production of thymine glycols in DNA by radiation and chemical carcinogens as detected by a monoclonal antibody. *Br. J. Cancer* 55 (Suppl.), 113–117.
- (25) Vaghef, H., Wisén A.-C., and Hellman, B. (1996) Demonstration of benzo(a)pyrene-induced DNA damage in mice by alkaline single cell gel electrophoresis: Evidence for strand breaks in liver but not in lymphocytes and bone marrow. *Pharmacol. Toxicol.* 78, 37–48.
- (26) Seike, K., Murata, M., Oikawa, S., Hiraku, Y., Hirakawa, K., Mimura, and Kawanishi, S. (2003) Oxidative DNA damage induced by benzo(a)anthracene metabolites via redox cycles of quinone and unique non-quinone. *Chem. Res. Toxicol.* 16, 1470–1476.
- (27) Miller, K. P., Chen, Y.-H., Hastings, V. L., Bral, C. M., and Ramos, K. S. (2000) Profiles of antioxidant/electrophile response element (ARE/EpRE) nuclear protein binding and *c*-Ha-ras transactivation in vascular smooth muscle cells treated with oxidative metabolites of benzo(a)pyrene. *Biochem. Pharmacol.* 60, 1285–1296.
- (28) Chesis, P. L., Levin, D. E., Smith, M. T., Ernster, L., and Ames, B. N. (1984) Mutagenicity of quinones: Pathways of metabolic activation and detoxification. *Proc. Natl. Acad. Sci. U.S.A.* 81, 1696–1700.
- (29) Flowers-Geary, L., Harvey, R. G., and Penning, T. M. (1993) Cytotoxicity of polycyclic hydrocarbon *o*-quinones in rat and human hepatoma cells. *Chem. Res. Toxicol.* 6, 252–260.
- (30) Staal, Y. C. M., van Herwijnen, M. H. M., van Schooten, F. J., and van Delft, J. H. M. (2006) Modulation of gene expression and DNA adduct formation in HepG2 cells by polycyclic aromatic hydrocarbons with different carcinogenic potencies. *Carcinogenesis* 27, 646–655.
- (31) Streitwieser, A., Jr., and Brown, S. M. (1988) Convenient preparation of 11H-benzo[a]fluorenone and 11H-benzo[b]fluorenone. *J. Org. Chem.* 53, 904–906.
- (32) Fieser, L. F., and Joshel, L. M. (1940) 9-Methyl-3,4-benzofluorene. *J. Am. Chem. Soc.* 62, 957–958.
- (33) Spijker, N. M., van den Braken-van Leersum, A. M., Lugtenburg, J., and Cornelisse, J. (1990) A very convenient synthesis of cyclopenta[*cd*]pyrene. *J. Org. Chem.* 55, 756–758.
- (34) Clar, E., and Mackay, C. C. (1972) Circobiphenyl and the attempted synthesis of 1:14, 3:4, 7:8, 10:11-tetrabenzoperopyrene. *Tetrahedron* 28, 6041–6047.
- (35) Adachi, J., Mori, Y., Matsui, S., and Matsuda, T. (2004) Comparison of gene expression patterns between 2,3,7,8-tetrachlorodibenzo-*p*-dioxin and a natural arylhydrocarbon receptor ligand, indirubin. *Toxicol. Sci.* 80, 161–169.
- (36) Iwanari, M., Nakajima, M., Kizu, R., Hayakawa, K., and Yokoi, T. (2002) Induction of CYP1A1, CYP1A2, and CYP1B1 mRNAs by nitropolycyclic aromatic hydrocarbons in various human tissue-derived cells: Chemical-, cytochrome P450 isoform-, and cell-specific differences. *Arch. Toxicol.* 76, 287–298.
- (37) Vakhara, D. D., Liu, N., Pause, R., Fasco, M., Bessette, E., Zhang, Q.-Y., and Kaminsky, L. S. (2001) Polycyclic aromatic hydrocarbon/metal mixtures: Effect on PAH induction of CYP1A1 in human HepG2 cells. *Drug Metab. Dispos.* 29, 999–1006.
- (38) Bessette, E., Fasco, M. J., Pentecost, T., and Kaminsky, L. S. (2005) Mechanisms of arsenite-mediated decreases in benzo[*k*]fluoranthene-induced human cytochrome P4501A1 Levels in HepG2 cells. *Drug Metab. Dispos.* 33, 312–320.
- (39) Jones, J. M., and Anderson, J. W. (1999) Relative potencies of PAHs and PCBs based on the response of human cells. *Environ. Toxicol. Pharmacol.* 7, 19–26.
- (40) Jones, J. M., Anderson, J. W., and Tukey, R. H. (2000) Using the metabolism of PAHs in a human cell line to characterize environmental samples. *Environ. Toxicol. Pharmacol.* 8, 119–126.
- (41) Lekas, P., Tin, K. L., Lee, C., and Prokipcak, R. D. (2000) The human cytochrome P450 1A1 mRNA in rapidly degraded in HepG2 cells. *Arch. Biochem. Biophys.* 384, 311–318.
- (42) Plakunov, I., Smolarek, T. A., Fischer, D. L., Wiley, J. C., Jr., and Baird, W. M. (1987) Separation by ion-pair high-performance liquid chromatography of the glucuronide, sulfate and glutathione conjugates formed from benzo[*a*]pyrene in cell cultures from rodents, fish and humans. *Carcinogenesis* 8, 59–66.
- (43) Nesnow, S., Ross, J. A., Mass, M. J., and Stoner, G. D. (1998) Mechanistic relationships between DNA adducts, oncogene mutations, and lung tumorigenesis in strain A mice. *Exp. Lung Res.* 24, 395–405.
- (44) Rice, J. E., Coleman, D. T., Hosted, T. J., Jr., LaVoie, E. J., and Wiley, J. C., Jr. (1985) Identification of mutagenic metabolites of indeno[1,2,3-*cd*]pyrene formed *in vitro* with rat liver enzymes. *Cancer Res.* 45, 5421–5425.
- (45) Monks, T. J., Hanzlik, R. P., Cohen, G. M., Ross, D., and Graham, D. G. (1992) Quinone chemistry and toxicity. *Toxicol. Appl. Pharmacol.* 112, 2–16.
- (46) Rowe, J. D., Nieves, E., and Listowsky, I. (1997) Subunit diversity and tissue distribution of human glutathione S-transferase: Interpretations based on electrospray ionization-MS and peptide sequence-specific antisera. *Biochem. J.* 325, 481–486.
- (47) Aninat, C., Piton, A., Glaise, D., Charpentier, T. L., Langouët, Morel, F., Guguen-Guillouzo, C., and Guillouzo, A. (2006) Expression of cytochromes P450, conjugating enzymes and nuclear receptors in human hepatoma HepaRG cells. *Drug Metab. Dispos.* 34, 75–83.
- (48) Sundberg, K., Dreij, K., Seidel, A., and Jernström, B. (2002) Glutathione conjugation and DNA adduct formation of dibenzo[*a,f*]pyrene and benzo[*a*]pyrene diol epoxides in V79 cells stably expressing different human glutathione transferases. *Chem. Res. Toxicol.* 15, 170–179.
- (49) Zhao, W., and Ramos, K. S. (1998) Cytotoxic response profiles of cultured rat hepatocytes to selected aromatic hydrocarbons. *Toxicol. in Vitro* 12, 175–182.

TX060197U

## Increased DNA Damage in ALDH2-Deficient Alcoholics

Tomonari Matsuda,\*† Hisatoshi Yabushita,† Robert A. Kanaly,† Shinya Shibutani,† and Akira Yokoyama§

Department of Technology and Ecology, Graduate School of Global Environmental Studies, Kyoto University, Kyoto, Japan, Department of Pharmacological Sciences, State University of New York, Stony Brook, New York, and National Hospital Organization Kurihama Alcoholism Center, Yokosuka, Japan

Received May 26, 2006

Drinking alcohol is a risk factor for cancers of the oral cavity, pharynx, larynx, and esophagus. Although many studies suggest that acetaldehyde, a major metabolite of orally ingested alcohol, plays a crucial role in cancer initiation, the link between the aldehyde dehydrogenase-2 (ALDH2) genotype and acetaldehyde-derived DNA damage has not yet been explored. We have developed a sensitive and quantitative method for detecting the acetaldehyde-derived DNA adducts, *N*<sup>2</sup>-ethyl-2'-deoxyguanosine (*N*<sup>2</sup>-Et-dG),  $\alpha$ -*S*- and  $\alpha$ -*R*-methyl- $\gamma$ -hydroxy-1,*N*<sup>2</sup>-propano-2'-deoxyguanosine ( $\alpha$ -*S*-Me- $\gamma$ -OH-PdG and  $\alpha$ -*R*-Me- $\gamma$ -OH-PdG), and *N*<sup>2</sup>-(2,6-dimethyl-1,3-dioxan-4-yl)-deoxyguanosine (*N*<sup>2</sup>-Dio-dG), by using liquid chromatography electrospray tandem mass spectrometry (LC/ESI-MS/MS) and stable-isotope internal standards. We determined the DNA adducts in 44 blood DNA samples from Japanese alcoholic patients. The levels of three acetaldehyde-derived DNA adducts, *N*<sup>2</sup>-Et-dG,  $\alpha$ -*S*-Me- $\gamma$ -OH-PdG, and  $\alpha$ -*R*-Me- $\gamma$ -OH-PdG, were significantly higher in alcoholics with the *ALDH2*\*1/2\*2 genotype compared to those with the *ALDH2*\*1/2\*1 genotype. *N*<sup>2</sup>-Dio-dG was not detected in any of the DNA samples analyzed. These results provide molecular evidence that the ALDH2 genotype affects the genotoxic damage caused by acetaldehyde.

### Introduction

Alcoholic beverages are a risk factor for several cancers including oral cavity, pharynx, larynx, and esophagus cancers (1). Acetaldehyde, an oxidized metabolite of ethanol, is suspected to be the ultimate carcinogen in alcohol-related cancers. Acetaldehyde reacts with DNA *in vitro*, resulting in the formation of DNA adducts, such as *N*<sup>2</sup>-ethyl-2'-deoxyguanosine (*N*<sup>2</sup>-Et-dG)<sup>1</sup> (2),  $\alpha$ -*S*- and  $\alpha$ -*R*-methyl- $\gamma$ -hydroxy-1,*N*<sup>2</sup>-propano-2'-deoxyguanosine ( $\alpha$ -*S*-Me- $\gamma$ -OH-PdG and  $\alpha$ -*R*-Me- $\gamma$ -OH-PdG), and *N*<sup>2</sup>-(2,6-Dimethyl-1,3-dioxan-4-yl)-deoxyguanosine (*N*<sup>2</sup>-Dio-dG) (3). The exposure of acetaldehyde to mammalian cells increases the frequency of sister chromatid exchanges and chromosomal aberrations (4, 5) and induces DNA interstrand-cross-links (6) and DNA-protein-cross-links (7). Acetaldehyde has shown in shuttle-vector pMY189 propagated in human cells to induce tandem base substitutions that are most likely produced via DNA-intrastrand cross-links (6). Inhalation of acetaldehyde significantly increased the incidence of nasal tumors (8). These experimental evidences suggested that acetaldehyde acts as a tumor initiator.

Most of the acetaldehyde generated during alcohol ingestion is eliminated by aldehyde dehydrogenase-2 (ALDH2) (9). The mutant *ALDH2*\*2 allele (Glu487Lys) encodes a catalytically inactive subunit (10). Because ALDH2 is a homotetrameric

enzyme, individuals with the *ALDH2*\*1/2\*2 genotype should have only 6.25% of the normal protein; other molecules containing one or more *ALDH2*\*2 subunits are considered to be inactive (11). Distribution of the *ALDH2*\*2 allele varies by race (12), and it is most prevalent among East Asians. Approximately 40% of Japanese have the *ALDH2*\*2 allele, but it is absent in Caucasians and Africans. When ALDH2 is inactive, the body fails to rapidly metabolize acetaldehyde, leading excessive accumulation. In fact, alcohol challenge tests showed that after drinking a small amount of ethanol (0.1 g/kg body weight), the average peak of blood acetaldehyde concentrations in *ALDH2*\*1/2\*2 individuals was five times greater than that of active *ALDH2*\*1/2\*1 homozygotes who consumed a moderate amount of ethanol (0.8 g/kg body weight) (13).

A link between the ALDH2 genotype and cancer rates has been suggested (14, 15), but no direct evidence exists. In the present study, we explored a relationship between the ALDH2 genotype and the formation of acetaldehyde-derived DNA adducts in the blood of 44 alcoholics. In order to quantify low levels of the DNA adducts, we employed a sensitive method using stable isotope dilution coupled with liquid chromatography electrospray tandem mass spectrometry (LC/ESI-MS/MS).

### Experimental Procedures

**Subjects and ALDH2 Genotyping.** The participants in this study were 44 cancer-free, male Japanese alcoholic patients. This study was approved by the Ethics Committee of the National Hospital Organization Kurihama Alcoholism Center of Japan, and informed consent was obtained from participating patients. Information on the subjects' drinking profiles and smoking habits was obtained from the patients as described previously (16). Subjects' blood samples were obtained on the day of admission for alcoholism treatment, and ALDH2 genotyping was performed on blood DNA by polymerase chain reaction/restriction fragment length polymorphism (PCR-RFLP) analysis as described previously (16).

\* Corresponding author. Phone: +81-75-753-5171. Fax: +81-75-753-3335. E-mail: matsuda@eden.env.kyoto-u.ac.jp.

† Kyoto University.

‡ State University of New York.

§ National Hospital Organization Kurihama Alcoholism Center.

<sup>1</sup> Abbreviations: HPLC, high performance liquid chromatography; LC/ESI-MS/MS, liquid chromatography electrospray tandem mass spectrometry; ALDH2, aldehyde dehydrogenase-2; *N*<sup>2</sup>-Et-dG, *N*<sup>2</sup>-ethyl-2'-deoxyguanosine;  $\alpha$ -Me- $\gamma$ -OH-PdG,  $\alpha$ -methyl- $\gamma$ -hydroxy-1,*N*<sup>2</sup>-propano-2'-deoxyguanosine; *N*<sup>2</sup>-Dio-dG, *N*<sup>2</sup>-(2,6-dimethyl-1,3-dioxan-4-yl)-2'-deoxyguanosine.

**Synthesis of DNA Adduct and Stable Isotope Standards.** Analytical standards of  $N^2$ -Et-dG were prepared as described by Vaca et al. (7). Two diastereoisomers of  $\alpha$ -Me- $\gamma$ -OH-PdG and two diastereoisomers of  $N^2$ -Dio-dG were prepared as described by Wang et al. (8). The [ $^{15}\text{N}_5$ ]-labeled adducts were also synthesized following previous methods (7, 8) using [ $^{15}\text{N}_5$ ]-dG instead of dG and employed as the internal standards for LC/MS/MS.

**Preparation of a Standard DNA Sample Containing  $N^2$ -Et-dG and  $\alpha$ -Me- $\gamma$ -OH-PdG.** To make  $N^2$ -Et-dG-containing DNA, calf thymus DNA (73  $\mu\text{g}$  in 100  $\mu\text{L}$ ) was mixed with 10  $\mu\text{L}$  of acetaldehyde and incubated at 37  $^\circ\text{C}$  for 1 h. This was followed by treatment with approximately 3 mg of  $\text{NaBH}_3\text{CN}$ , and the mixture was incubated for another hour at 37  $^\circ\text{C}$ , yielding DNA containing  $N^2$ -Et-dG lesions. A similar approach was used to make calf thymus DNA containing  $\alpha$ -S-Me- $\gamma$ -OH-PdG and  $\alpha$ -R-Me- $\gamma$ -OH-PdG except that the DNA was reacted with 10  $\mu\text{L}$  of crotonaldehyde and incubated for 2 h, and the reduction by  $\text{NaBH}_3\text{CN}$  was unnecessary. The DNA samples were ethanol precipitated and gel-filtrated by using MicroSpin G-25 Columns (Amersham Biosciences, U.K.) mixed with untreated calf thymus DNA, and the final standard concentrations were determined as indicated in the Results section.

**Isolation of DNA from Blood and Digestion with Internal Standards.** DNA isolation was performed by the QIAamp DNA Blood Midi Kit (QIAGEN, Hilden, Germany). Blood DNA samples (20  $\mu\text{g}$ ) were digested to their corresponding 2'-deoxyribonucleoside-3'-monophosphates by the addition of 15  $\mu\text{L}$  of 17 mM citrate plus 8 mM  $\text{CaCl}_2$  buffer that contained micrococcal nuclease (22.5 units) and spleen phosphodiesterase (0.075 units) plus internal standards. Solutions were mixed and incubated for 3 h at 37  $^\circ\text{C}$ , after which alkaline phosphatase (3 units), 10  $\mu\text{L}$  of 0.5 M Tris HCl (pH 8.5), 5  $\mu\text{L}$  of 20 mM  $\text{ZnSO}_4$ , and 67  $\mu\text{L}$  distilled water were added and incubated further for 3 h at 37  $^\circ\text{C}$ . The digested sample was extracted twice with methanol. The methanol fractions were evaporated to dryness, resuspended in 100  $\mu\text{L}$  of distilled water, and subjected to LC/ESI-MS/MS.

**Instrumentation.** LC/ESI-MS/MS analyses were performed using a Shimadzu LC system (Shimadzu) interfaced with a Quattro Ultima triple stage quadrupole MS (Waters-Micromass, Manchester, U.K.). The LC column was eluted over a gradient that began at a ratio of 2% methanol to 98% water and was changed to 40% methanol over a period of 40 min, changed to 80% methanol from 40 to 45 min, and finally returned to the original starting conditions, 2:98, for the remaining 15 min. The total run time was 60 min. Sample injection volumes of 50  $\mu\text{L}$  each were separated on a Shim-pack FC-ODS column (4.6  $\times$  150 mm; Shimadzu, Japan) and eluted at a flow rate of 0.4 mL/min. Mass spectral analyses were carried out in positive ion mode with nitrogen as the nebulizing gas. The ion source temperature was 130  $^\circ\text{C}$ , the desolvation gas temperature was 380  $^\circ\text{C}$ , and the cone voltage was operated at a constant 35 V. Nitrogen gas was also used as the desolvation gas (700 L/h), and cone gas (35 L/h) and argon were used as the collision gas at a collision cell pressure of  $1.5 \times 10^{-3}$  mBar. Positive ions were acquired in MRM mode. The MRM transitions monitored were as follows:  $N^2$ -Dio-dG,  $m/z$  382  $\rightarrow$  266; [ $^{15}\text{N}_5$ ]- $\alpha$ -Me- $\gamma$ -OH-PdG,  $m/z$  343  $\rightarrow$  227;  $\alpha$ -Me- $\gamma$ -OH-PdG,  $m/z$  338  $\rightarrow$  222; [ $^{15}\text{N}_5$ ]- $N^2$ -Et-dG,  $m/z$  301  $\rightarrow$  185;  $N^2$ -Et-dG,  $m/z$  296  $\rightarrow$  180. The amount of each DNA adduct was quantified by the ratio of the peak area of the target adducts and of its stable isotope (stable isotope-dilution method). QuanLynx (ver. 4.0) software (Waters-Micromass, Manchester, U.K.) was used to create standard curves and calculate the adduct concentrations. The amount of deoxyguanosine (dG) was monitored by a Shimadzu SPD-10A UV-Visible detector that was in place before the tandem mass spectrometer. The adduct level is shown as femtomoles of adducts per micromoles of dG. The number of DNA adducts per  $10^9$  bases was calculated by the following equation: Number of DNA adducts per  $10^9$  bases = adduct level (fmol/ $\mu\text{mol}$  dG)  $\times$  0.218 ( $\mu\text{mol}$  dG/ $\mu\text{mol}$  dN), where 0.218 is the average ratio of guanine bases relative to total base number in human blood DNA calculated from this experiment (data not shown).

**Table 1. Genotype, Age and Drinking and Smoking Habits of 44 Japanese Alcoholics<sup>a</sup>**

ALDH2 genotype	n	age (years)	ethanol (g/day)	duration of drinking (years)	cigarettes (no/day)
2*1/2*1	19	52 $\pm$ 11	130 $\pm$ 54	26 $\pm$ 13	22 $\pm$ 13
2*1/2*2	25	51 $\pm$ 11	105 $\pm$ 59	24 $\pm$ 12	24 $\pm$ 15

<sup>a</sup> Information was obtained from patients and, when available, their partners upon admission to the program. The information included the daily alcohol consumption during the year preceding admission, the duration of habitual drinking, and the daily number of cigarettes currently smoked. Daily alcohol consumption was expressed in grams per day of ethanol using standard conversion for alcoholic beverages: beer was considered to be 5% ethanol (v/v); wine, 12%; sake, 16%; shochu, 25%; and whiskey, 40%.

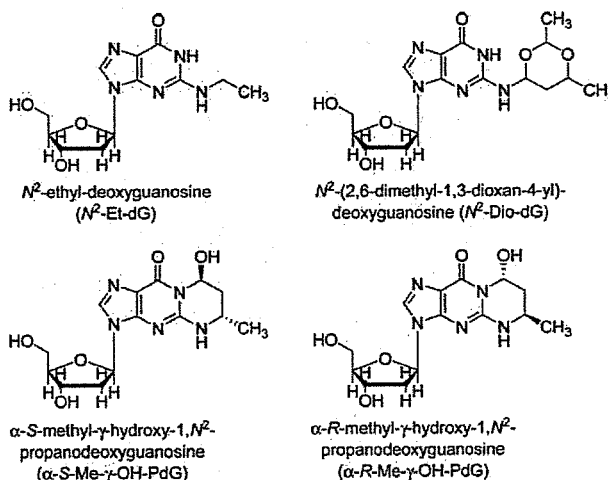


**Figure 1.** Structure of DNA adducts induced by acetaldehyde.

## Results

We enrolled 19 alcoholic patients with the  $ALDH2^{*1/2*1}$  genotype and 25 alcoholic patients with the  $ALDH2^{*1/2*2}$  genotype. The averages of age, daily ethanol consumption, duration of drinking, and daily cigarette consumption were not significantly different between the  $ALDH2$  genotypes (Table 1).

Figure 2 shows the MS/MS chromatogram (raw data, without smoothing) of five acetaldehyde-derived DNA adduct standards: two diastereoisomers of  $N^2$ -Dio-dG, two diastereoisomers of  $\alpha$ -Me- $\gamma$ -OH-PdG, and  $N^2$ -Et-dG. The amount of injection on column, for each, was 250 fg, corresponding to 2 to 3 adducts per  $10^8$  bases in 10  $\mu\text{g}$  of DNA. Sufficient signal-to-noise ratios was observed in each peak, indicating the high sensitivity of this analysis.

To make a standard DNA solution containing  $N^2$ -Et-dG and  $\alpha$ -Me- $\gamma$ -OH-PdG, acetaldehyde-treated and crotonaldehyde-treated calf thymus DNA and untreated calf thymus DNA were mixed in proper proportions. Then, 10 fmol each of the three stable isotope standards, [ $^{15}\text{N}_5$ ]- $N^2$ -Et-dG, [ $^{15}\text{N}_5$ ]- $\alpha$ -S-Me- $\gamma$ -OH-PdG, and [ $^{15}\text{N}_5$ ]- $\alpha$ -R-Me- $\gamma$ -OH-PdG, were spiked into 20  $\mu\text{g}$  of the standard DNA and enzymatically digested to deoxynucleosides; half of the digests were subjected to LC/ESI-MS/MS analysis. Repeated analysis (eight times) of the same standard DNA gave  $613 \pm 52$  fmol/ $\mu\text{mol}$  dG (CV = 8.5%),  $592 \pm 40$  fmol/ $\mu\text{mol}$  dG (CV = 6.7%), and  $845 \pm 81$  fmol/ $\mu\text{mol}$  dG (CV = 9.6%) for  $N^2$ -Et-dG,  $\alpha$ -S-Me- $\gamma$ -OH-PdG, and  $\alpha$ -R-Me- $\gamma$ -OH-PdG, respectively.

Next, the DNA samples extracted from the blood of the 44 alcoholics were analyzed by the same procedures. Representative chromatograms of acetaldehyde-derived DNA adducts in blood

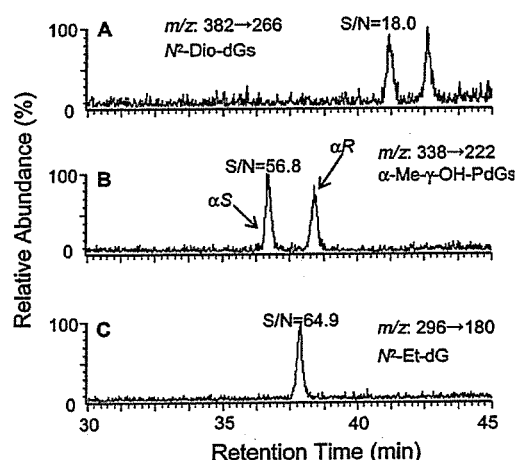


**Figure 2.** MS/MS chromatograms of five acetaldehyde-derived DNA adduct standards. (A) Two diastereomers of  $N^2$ -Dio-dG ( $m/z$ : 382  $\rightarrow$  266); (B) two diastereomers of  $\alpha$ -Me- $\gamma$ -OH-PdG ( $m/z$ : 338  $\rightarrow$  222); (C)  $N^2$ -Et-dG ( $m/z$ : 296  $\rightarrow$  180). A Quattro Ultima Pt triple stage quadrupole MS spectrometer was used. The analytical settings are as described in Experimental Procedures. Fifty microliters of each 5 pg/mL solution of a 5-adduct mixture was injected (250 fg on column). The signal-to-noise ratio (S/N) was calculated by using the MassLynx (ver 4.0) software.

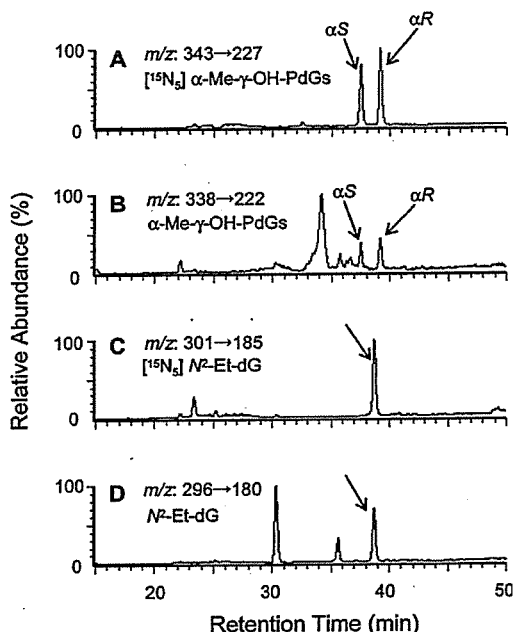


**Figure 3.** LC/ESI-MS/MS detection of acetaldehyde-derived DNA adducts from human blood. Stable isotope internal standards [ $^{15}\text{N}_5$ ]- $\alpha$ -S- and  $\alpha$ -R-Me- $\gamma$ -OH-PdG (A) and [ $^{15}\text{N}_5$ ]- $N^2$ -Et-dG (C) were spiked into DNA samples and monitored at transitions  $m/z$  343  $\rightarrow$  227 and 301  $\rightarrow$  185 as indicated and were used for the unambiguous confirmation of  $\alpha$ -S- and  $\alpha$ -R-Me- $\gamma$ -OH-PdG (B) and  $N^2$ -Et-dG (D) at transitions  $m/z$  338  $\rightarrow$  222 and 296  $\rightarrow$  180. In the sample shown in the Figure,  $N^2$ -Et-dG,  $\alpha$ -S-, and  $\alpha$ -R-Me- $\gamma$ -OH-PdG were detected at levels of 51, 8, and 13 adducts per  $10^9$  bases, respectively, illustrating the sensitivity of the method.

DNA are shown in Figure 3. The peaks of  $N^2$ -Et-dG,  $\alpha$ -S-Me- $\gamma$ -OH-PdG, and  $\alpha$ -R-Me- $\gamma$ -OH-PdG were clearly observed at the same retention time as that of their stable isotope internal standards. Peaks corresponding to  $N^2$ -Dio-dG were not detected in any of the samples analyzed.

We found that the average levels of three acetaldehyde-derived adducts were significantly higher in  $ALDH2^{*1/2*2}$

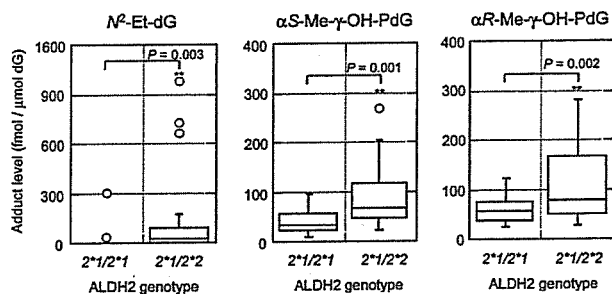


**Figure 4.** Box plots illustrating that the average levels of three acetaldehyde-derived adducts were significantly higher in the blood DNA of alcoholics who possessed the  $ALDH2^{*1/2*2}$  genotype compared to alcoholics who possessed the  $ALDH2^{*1/2*1}$  genotype. The  $P$  values are given for the Wilcoxon-Mann-Whitney test ( $N^2$ -Et-dG) and  $t$ -test ( $\alpha$ -Me- $\gamma$ -OH-PdGs).

alcoholics.  $N^2$ -Et-dG was detected in 14 out of 25 blood DNA samples from the  $ALDH2^{*1/2*2}$  alcoholics but in only 2 out of 19 from the  $ALDH2^{*1/2*1}$  alcoholics. The average level of  $N^2$ -Et-dG in the blood samples from the  $ALDH2^{*1/2*2}$  alcoholic patients (average  $\pm$  SEM:  $130 \pm 52$  fmol/ $\mu$ mol dG,  $n = 25$ ) was significantly higher than that from the  $ALDH2^{*1/2*1}$  alcoholics ( $17.8 \pm 15.9$  fmol/ $\mu$ mol dG,  $n = 19$ ) (Figure 4).  $\alpha$ -S-Me- $\gamma$ -OH-PdG and  $\alpha$ -R-Me- $\gamma$ -OH-PdG adducts were also detected in all analyzed blood samples. As was shown for  $N^2$ -Et-dG, the levels of  $\alpha$ -S-Me- $\gamma$ -OH-PdG and  $\alpha$ -R-Me- $\gamma$ -OH-PdG in DNA samples from the  $ALDH2^{*1/2*2}$  alcoholics (average  $\pm$  SEM:  $92.4 \pm 12.9$  and  $114 \pm 15$  fmol/ $\mu$ mol dG,  $n = 25$ ) were also significantly higher than those of the  $ALDH2^{*1/2*1}$  alcoholics ( $42.9 \pm 6.0$  and  $61.3 \pm 6.4$ ,  $n = 19$ ) (Figure 4).

## Discussion

Using stable isotope internal standards, we determined acetaldehyde-derived DNA adducts,  $N^2$ -Et-dG,  $\alpha$ -Me- $\gamma$ -OH-PdG, and  $N^2$ -Dio-dG, in the blood DNA of alcoholic patients by LC/ESI-MS/MS.  $N^2$ -Et-dG and  $\alpha$ -Me- $\gamma$ -OH-PdG were detected; however,  $N^2$ -Dio-dG was not detected in any of the blood DNA samples. Because  $N^2$ -Dio-dG is produced from three acetaldehyde molecules, a high concentration of acetaldehyde may be required in the human body to form this adduct.

The reaction of acetaldehyde with dG results in the formation of an unstable Schiff base at the  $N^2$  position of dG ( $N^2$ -ethylidene-dG). The formation of the stable  $N^2$ -Et-dG adduct requires a subsequent reduction step that must be accomplished by some reducing agent such as vitamin C, glutathione, and so forth. Using a  $^{32}\text{P}$ -postlabeling procedure in combination with HPLC-radioisotope detection, Fang and Vaca (7) detected 2 to 3 adducts per  $10^7$  bases of  $N^2$ -Et-dG in white blood cell DNA obtained from Swedish alcoholic patients. In the present study, we found, using a more reliable LC/ESI-MS/MS and internal standards, that the average level of blood  $N^2$ -Et-dG adducts in  $ALDH2^{*1/2*2}$  and  $ALDH2^{*1/2*1}$  alcoholics were 28.3 and 3.9 adducts per  $10^9$  bases, respectively; the level was at least 1 or 2 orders of magnitude lower in Japanese alcoholic patients than that observed with the Swedish alcoholic patients by  $^{32}\text{P}$ -postlabeling. This year, Wang et al. (17) showed that  $N^2$ -ethylidene-dG in human liver DNA is relatively stable and that the presence of this adduct could be confirmed by the detection of  $N^2$ -Et-dG after the reduction of DNA during isolation and enzymatic hydrolysis. They showed that when the reduction step was included during these steps approximately a few 100 times more  $N^2$ -Et-dG was detected in some cases. Although the biological significance of  $N^2$ -ethylidene-dG has not yet been

determined, this new adduct may be a good biomarker to evaluate exposure to acetaldehyde, and we will consider evaluating this adduct in future studies.

The mutagenicity of *N*<sup>2</sup>-Et-dG has been reported previously (15). The primer extension assay using site-specifically modified oligodeoxynucleotides containing a single *N*<sup>2</sup>-Et-dG revealed that dGMP is incorporated opposite the *N*<sup>2</sup>-Et-dG adduct during DNA synthesis and is catalyzed by the *Escherichia coli* DNA polymerase I Klenow fragment (40% of fully extended primer contained dGMP opposite to *N*<sup>2</sup>-Et-dG in template), indicating that this adduct induces G to C mutations (18). *N*<sup>2</sup>-Ethyl-2'-deoxyguanosine triphosphate (*N*<sup>2</sup>-Et-dGTP) was effectively utilized during DNA synthesis catalyzed by mammalian DNA polymerases  $\alpha$  and  $\delta$  (19). *N*<sup>2</sup>-Et-dG strongly blocks polymerization of DNA polymerase  $\alpha$ , but DNA polymerase  $\eta$  bypassed the lesion in an error-free manner (20). However, miscoding and the mutagenic potential of the *N*<sup>2</sup>-Et-dG adduct have not so far been extensively explored in mammalian cells.

The exposure of DNA to acetaldehyde *in vitro* resulted in the formation of  $\alpha$ -*S*-Me- $\gamma$ -OH-PdG and  $\alpha$ -*R*-Me- $\gamma$ -OH-PdG (8). The formation of  $\alpha$ -Me- $\gamma$ -OH-PdGs via acetaldehyde is facilitated by basic amino acids, such as arginine and lysine, histones, or polyamines, such as spermine and spermidine, indicating the possibility of the formation of these adducts by acetaldehyde *in vivo* (21, 22). When a single-strand shuttle vector containing a single diastereoisomer of  $\alpha$ -Me- $\gamma$ -OH-PdG was propagated in a mammalian cell line (23), the mutational frequency was 5 to 6%; G to T transversions were dominantly detected. In addition,  $\alpha$ -Me- $\gamma$ -OH-PdGs are thought to be the precursor lesions to DNA-DNA or DNA-protein cross-links. In the nucleoside form or in single-stranded DNA,  $\alpha$ -Me- $\gamma$ -OH-PdGs exist in cyclic form. However, in double-stranded DNA, the ring-opened form of the lesion containing a free aldehyde group is dominant. Kozekov et al. (24) demonstrated that double-stranded oligonucleotides that contain a single  $\alpha$ -*S*-Me- $\gamma$ -OH-PdG or  $\alpha$ -*R*-Me- $\gamma$ -OH-PdG spontaneously formed DNA interstrand cross-links. The reaction of forming DNA interstrand cross-links was very slow, taking a few days to a few weeks, although the reaction with  $\alpha$ -*R*-Me- $\gamma$ -OH-PdG was significantly faster than that with  $\alpha$ -*S* diastereomer. When double stranded oligonucleotides containing a single  $\alpha$ -*S*-Me- $\gamma$ -OH-PdG or  $\alpha$ -*R*-Me- $\gamma$ -OH-PdG were mixed with the peptide (Lys-Trp-Lys-Lys), the DNA-protein cross-links were also formed (25) within an hour. DNA interstrand cross-links and DNA-protein cross-links have been documented in acetaldehyde-exposed mammalian cells and may lead to chromosomal aberrations and sister chromatid exchanges.  $\alpha$ -Me- $\gamma$ -OH-PdG adducts may contribute to the development of alcohol-induced cancers.

Studies of various Japanese drinking populations have shown that deficient ALDH2 encoded by the *ALDH2*\*1/2\*2 genotype is a high risk factor for esophageal cancer. For example, heavy drinkers with the *ALDH2*\*1/2\*2 genotype have a high odd ratio (16.4) of getting esophageal cancer (14). We demonstrated that the level of acetaldehyde-derived DNA adducts in the alcoholics with the *ALDH2*\*1/2\*2 genotype is much higher than that in alcoholics with the *ALDH2*\*1/2\*1 genotype. Our results strongly indicate that the ALDH2 genotype plays a crucial role in the formation of acetaldehyde-derived DNA adducts.

Ishikawa et al. demonstrated that micronuclei frequency in peripheral blood lymphocytes of ALDH2-deficient habitual drinkers were slightly, but significantly higher than that of ALDH2-proficient habitual drinkers (26). Morimoto and Takeshita reported that lymphocytes from habitual drinkers with

the deficient ALDH2 enzyme had significantly higher frequencies of sister chromatid exchanges than those from ALDH2-proficient individuals (27). These observations suggest that the ALDH2 genotype may affect the risk of cancer initiation by acetaldehyde in humans. In this study, we showed more direct evidence that the formation of acetaldehyde-derived DNA adducts, *N*<sup>2</sup>-Et-dG and  $\alpha$ -Me- $\gamma$ -OH-PdG, was closely related to the ALDH2 genotype in populations that are continuously exposed to high levels of acetaldehyde by alcohol consumption. Taken together, the observations from biochemical, epidemiological, and molecular epidemiological studies discussed above, in conjunction with this study, well fit the scenario that acetaldehyde is a primary causative factor for alcohol-induced cancers.

**Acknowledgment.** This research was supported in part by Grants-in-aid for Cancer Research from the Ministry of Health, Labor and Welfare of Japan and Grants-in-aid for Scientific Research from the Ministry of Education, Culture, Sports, Science and Technology of Japan.

## References

- (1) IARC (1988) Alcohol Drinking. *IARC Monograph on the Evaluation of the Carcinogenic Risk to Humans*, Vol. 44, pp 153-246, IARC, Lyon, France.
- (2) Fang, J. L., and Vaca, C. (1997) Detection of DNA adducts of acetaldehyde in peripheral white blood cells of alcohol abusers. *Carcinogenesis* 18, 627-632.
- (3) Wang, M., McIntee, E. J., Cheng, G., Shi, Y., Villalta, P. W., and Hecht, S. S. (2000) Identification of DNA adducts of acetaldehyde. *Chem. Res. Toxicol.* 13, 1149-1157.
- (4) Obe, G., Natarajan, A. T., Meyers, M., and Hertog, A. D. (1979) Induction of chromosomal aberrations in peripheral lymphocytes of human blood *in vitro*, and SCEs in bone-marrow cells of mice *in vivo* by ethanol and its metabolite acetaldehyde. *Mutat. Res.* 68, 291-294.
- (5) Obe, G., and Ristow, H. (1977) Acetaldehyde, but not ethanol, induces sister chromatid exchanges in Chinese hamster cells *in vitro*. *Mutat. Res.* 56, 211-213.
- (6) Matsuda, T., Kawanishi, M., Yage, T., Matsui, S., and Takebe, H. (1998) Specific tandem GG to TT base substitutions induced by acetaldehyde are due to intra-strand crosslinks between adjacent guanine bases. *Nucleic Acids Res.* 26, 1769-1774.
- (7) Kuykendall, J. R., and Bogdanffy, M. S. (1992) Efficiency of DNA-histone crosslinking induced by saturated and unsaturated aldehydes *in vitro*. *Mutat. Res.* 283, 131-136.
- (8) IARC (1985) Allyl Compounds, Aldehydes, Epoxides and Peroxides. *IARC Monograph on the Evaluation of the Carcinogenic Risk to Humans*, Vol. 36, pp 101-132, IARC, Lyon, France.
- (9) Bosron, W. F., and Li, T. K. (1986) Genetic polymorphism of human liver alcohol and aldehyde dehydrogenases, and their relationship to alcohol metabolism and alcoholism. *Hepatology* 6, 502-510.
- (10) Yoshida, A., Hsu, L., and Yasunami, M. (1991) Genetics of human alcohol-metabolizing enzymes. *Prog. Nucleic Acids Res. Mol. Biol.* 40, 255-287.
- (11) Crabb, D. W., Edenberg, H. J., Bosron, W. F., and Li, T. K. (1989) Genotype for aldehyde dehydrogenase deficiency and alcohol sensitivity: the inactive ALDH2 allele is dominant. *J. Clin. Invest.* 83, 314-316.
- (12) Goedde, H. W., Agarwal, D. P., Fritze, G., et al. (1992) Distribution of ADH2 and ALDH2 genotypes in different populations. *Hum. Genet.* 88, 344-346.
- (13) Enomoto, N., Takase, S., Yasuhara, M., and Takada, A. (1991) Acetaldehyde metabolism in different aldehyde dehydrogenase-2 genotypes. *Alcohol Clin. Exp. Res.* 15, 141-144.
- (14) Yokoyama, A., and Omori, T. (2003) Genetic polymorphisms of alcohol and aldehyde dehydrogenases and risk for esophageal and head and neck cancers. *Jpn. J. Clin. Oncol.* 33, 111-121.
- (15) Brooks, P., and Theruvathu, J. A. (2005) DNA adducts from acetaldehyde: implications for alcohol-related carcinogenesis. *Alcohol* 35, 187-193.
- (16) Yokoyama, A., Muramatsu, T., Ohmori, T., Yokoyama, T., Okuyama, K., Takahashi, H., Hasegawa, Y., Higuchi, S., Maruyama, K., Shirakura, K., and Ishii, H. (1998) Alcohol-related cancers and aldehyde dehydrogenase-2 in Japanese alcoholics. *Carcinogenesis* 19, 1383-1387.

- (17) Wang, M., Nanxiong, Y., Li, C., Villalta, P. W., Hochalter, J. B., and Hecht, S. S. (2006) Identification of an acetaldehyde adduct in human liver DNA and quantitation as *N*<sup>2</sup>-ethyldeoxyguanosine. *Chem. Res. Toxicol.* 19, 319–324.
- (18) Terashima, I., Matsuda, T., Fang, T., Suzuki, N., Kobayashi, J., Kohda, K., and Shibutani, S. (2001) Miscoding potential of the *N*<sup>2</sup>-ethyl-2'-deoxyguanosine DNA adduct by the exonuclease free Klenow fragment of *Escherichia coli* DNA polymerase I. *Biochemistry* 40, 4106–4114.
- (19) Matsuda, T., Terashima, I., Matsumoto, Y., Yabushita, H., Matsui, S., and Shibutani, S. (1999) Effective utilization of *N*<sup>2</sup>-ethyl-2'-deoxyguanosine triphosphate during DNA synthesis catalyzed by mammalian replicative DNA polymerases. *Biochemistry* 38, 929–935.
- (20) Perrino, F. W., Blans, P., Harvey, S., Gelhaus, S. L., McGrath, C., Akman, S. A., Jenkins, G. S., LaCourse, W. R., and Fishbein, J. C. (2003) The *N*<sup>2</sup>-ethylguanine and the O<sup>6</sup>-ethyl- and O<sup>6</sup>-methylguanine lesions in DNA: Contrasting responses from the "bypass" DNA polymerase  $\eta$  and the replicative DNA polymerase  $\alpha$ . *Chem. Res. Toxicol.* 16, 1616–1623.
- (21) Sako, M., Inagaki, S., Esaka, Y., and Deyashiki, Y. (2003) Histones accelerate the cyclic 1, *N*<sup>2</sup>-propanoguanine adduct-formation of DNA by the primary metabolite of alcohol and carcinogenic crotonaldehyde. *Bioorg. Med. Chem. Lett.* 13, 3497–3498.
- (22) Theruvathu, J. A., Jaruga, P., Nath, R. G., Dizdaroglu, M., and Brooks, P. J. (2005) Polyamines stimulate the formation of mutagenic 1, *N*<sup>2</sup>-propanodeoxyguanosine adducts from acetaldehyde. *Nucleic. Acids. Res.* 33, 3513–3520.
- (23) Fernandes, P., Kanuri, M., Nechev, L. V., Harris, T. M., and Lloyd, R. S. (2005) Mammalian cell mutagenesis of the DNA adducts of vinyl chloride and crotonaldehyde. *Environ. Mol. Mutagen.* 45, 455–459.
- (24) Kozekov, I. D., Nechev, L. V., Moseley, M. S., Harris, C. M., Rizzo, C. J., Stone, M. P., and Harris, T. M. (2002) DNA interchain cross-links formed by acrolein and crotonaldehyde. *J. Am. Chem. Soc.* 125, 50–61.
- (25) Kurtz, A. J., and Lloyd, R. S. (2003) 1, *N*<sup>2</sup>-Deoxyguanosine adducts of acrolein, crotonaldehyde, and trans-4-hydroxynonenal cross-link to peptides via schiff base linkage. *J. Biol. Chem.* 278, 5970–5976.
- (26) Ishikawa, H., Yamamoto, H., Tian, Y., Kawano, M., Yamauchi, T., and Yokoyama, K. (2003) Effects of ALDH2 gene polymorphisms and alcohol-drinking behavior on micronuclei frequency in non-smokers. *Mutat. Res.* 541, 71–80.
- (27) Morimoto, K., and Takeshita, T. (1996) Low Km aldehyde dehydrogenase (ALDH2) polymorphism, alcohol-drinking behavior, and chromosome alterations in peripheral lymphocytes. *Environ. Health Perspect.* 104, 563–567.

TX060113H





## Combined genotoxic effects of radiation and a tobacco-specific nitrosamine in the lung of *gpt* delta transgenic mice

Megumi Ikeda<sup>a,b</sup>, Ken-ichi Masumura<sup>a</sup>, Yasuteru Sakamoto<sup>a</sup>, Bing Wang<sup>c</sup>,  
Mitsuru Neno<sup>c</sup>, Keiko Sakuma<sup>b</sup>, Isamu Hayata<sup>c</sup>, Takehiko Nohmi<sup>a,\*</sup>

<sup>a</sup> Division of Genetics and Mutagenesis, National Institute of Health Sciences, 1-18-1 Kamiyoga, Setagaya-ku, Tokyo 158-8501, Japan

<sup>b</sup> Graduate School of Nutrition and Health Sciences, Kagawa Nutrition University, 3-9-21 Chiyoda, Sakado-shi, Saitama 350-0288, Japan

<sup>c</sup> Radiation Effect Mechanisms Research Group, Research Center of Radiation Protection, National Institute of Radiological Sciences, 4-9-1 Anagawa, Inage-ku, Chiba-shi, Chiba 263-8555, Japan

Received 22 May 2006; received in revised form 25 July 2006; accepted 31 July 2006

Available online 7 September 2006

### Abstract

It is important to evaluate the health effects of low-dose-rate or low-dose radiation in combination with chemicals as humans are exposed to a variety of chemical agents. Here, we examined combined genotoxic effects of low-dose-rate radiation and 4-(methylnitrosamino)-1-(3-pyridyl)-1-butanone (NNK), the most carcinogenic tobacco-specific nitrosamine, in the lung of *gpt* delta transgenic mice. In this mouse model, base substitutions and deletions can be separately analyzed by *gpt* and *Spi*<sup>-</sup> selections, respectively. Female *gpt* delta mice were either treated with  $\gamma$ -irradiation alone at a dose rate of 0.5, 1.0 or 1.5 mGy/h for 22 h/day for 31 days or combined with NNK treatments at a dose of 2 mg/mouse/day, i.p. for four consecutive days in the middle course of irradiation. In the *gpt* selection, the NNK treatments enhanced the mutation frequencies (MFs) significantly, but no obvious combined effects of  $\gamma$ -irradiation were observable at any given radiation dose. In contrast, NNK treatments appeared to suppress the *Spi*<sup>-</sup> large deletions. In the *Spi*<sup>-</sup> selection, the MFs of deletions more than 1 kb in size increased in a dose-dependent manner. When NNK treatments were combined, the dose–response curve became bell-shaped where the MF at the highest radiation dose decreased substantially. These results suggest that NNK treatments may elicit an adaptive response that eliminates cells bearing radiation-induced double-strand breaks in DNA. Possible mechanisms underlying the combined genotoxicity of radiation and NNK are discussed, and the importance of evaluation of combined genotoxicity of more than one agent is emphasized.

© 2006 Elsevier B.V. All rights reserved.

**Keywords:** Combined genotoxic effects; Radiation; NNK; Lung cancer; *gpt* delta mice; Deletion

### 1. Introduction

Environmental factors play important roles in the etiology of human cancer [1]. Of various environmental hazardous compounds, cigarette smoke is the

most causative factor associated with the increase in cancer risk in humans. Tobacco smoking plays a major role in the etiology of lung, oral cavity and esophageal cancers, and a variety of chronic degenerative diseases [2]. Although cigarette smoke is a mixture of about 4000 chemicals including more than 60 known human carcinogens, 4-(methylnitrosamino)-1-(3-pyridyl)-1-butanone (nicotine-derived nitrosamino ketone, NNK) is the most carcinogenic tobacco-specific nitrosamine [3,4]. NNK induces lung tumors in mice,

\* Corresponding author. Tel.: +81 3 3700 9873;  
fax: +81 3 3707 6950.  
E-mail address: [nohmi@nih.go.jp](mailto:nohmi@nih.go.jp) (T. Nohmi).

rats and hamsters, and International Agency for Research on Cancer has concluded that exposure to NNK and NNN (*N*'-nitrosonornicotine) is carcinogenic to humans [5]. NNK is metabolically activated by CYP (P-450) enzymes in the lung and generates *O*<sup>6</sup>-methylguanine in DNA, which leads to G:C to A:T mutations, and the subsequent activation of *Ki-ras* proto-oncogene, an initiation of tumor development [6,7].

Radiation, on the other hand, is one of the most causative physical factors that induce human cancer. Radiation induces double-strand breaks (DSBs) in DNA, which lead to chromosome aberrations and cell deaths, and generates a variety of oxidative DNA damage [8]. Because of the genotoxicity, radiation at high doses clearly induces various tumors in humans [9]. Even at low doses, residential exposure to radioactive radon and its decay products may account for about 10% of all lung cancer deaths in the United States and about 20% of the lung cancer cases in Sweden [10,11].

Since humans are exposed to a variety of chemical and physical agents that may induce cancer, these factors may interact with each other and the action of one agent may be influenced by exposure to another agent [12]. The risk from combined exposure to more than one agent may be substantially higher or lower than predicted from the sum of the individual agents. In fact, low-dose radiation can induce an adaptive response, causing rodent or human cells to become resistant to genotoxic damage by subsequent higher doses of radiation [13]. Pre-exposure to alkylating agents at low doses induces another adaptive response that provides mechanisms by which the exposed bacterial cells can tolerate the higher challenging doses of genotoxic agents [14]. In addition, mitomycin C, bleomycin, hydrogen peroxide, metals and quercetin may also induce an adaptive response [15].

To explore the mechanisms underlying the interactive effects of chemical and physical agents on carcinogenesis, we examined the combined genotoxic effects of NNK and  $\gamma$ -irradiation in the lung of *gpt* delta transgenic mice [16]. In this mouse model, point mutations and deletions are separately analyzable by *gpt* and *Spi*<sup>-</sup> selections, respectively [17]. Point mutations such as base substitutions are induced by a number of chemical carcinogens including NNK [18]. *Spi*<sup>-</sup> selection detects deletions in size between 1 bp and 10 kb [19]. Deletions in size more than 1 kb, which we call large deletions in this study, are efficiently induced by  $\gamma$ -ray, X-ray and carbon-ion irradiation [20], and are thought to be generated by non-homologous end joining (NHEJ) of DSBs in DNA [21].

We report here that low-dose-rate  $\gamma$ -irradiation enhanced the mutation frequencies (MFs) of the large

deletions in the lung of *gpt* delta mice in a dose-dependent manner. When combined with NNK treatments, however, the MF at the highest radiation dose, i.e., 1.02 Gy, was reduced by more than 50%, suggesting that NNK treatments may induce an adaptive response against radiation-induced deletion mutations. We discuss possible mechanisms of the adaptive response and emphasize the importance of the risk assessment of combined genotoxic effects of radiation and chemicals in vivo.

## 2. Materials and methods

### 2.1. Treatment of mice

*gpt* delta C57BL/6J transgenic mice were maintained in the conventional animal facility of National Institute of Radiological Sciences, Chiba, Japan, according to the institutional animal care guidelines. They were housed in autoclaved aluminum cages with sterile wood chips for bedding and given free access to standard laboratory chow (MB-1, Funabashi Farm Co., Japan) and acidified water under controlled lighting (12 h light/dark cycle). Seven-week-old female *gpt* delta mice were divided to eight groups each consisting of six mice. Three groups were  $\gamma$ -irradiated at a dose rate of 0.5, 1.0 or 1.5 mGy/h for 22 h/day for 2 weeks (Fig. 1). After the irradiation, three groups of mice were treated with a single i.p. injection of NNK (Toronto Research Chemicals, Toronto, Canada) dissolved in saline at a daily dose of 2 mg/mouse for four consecutive days. The irradiation continued during the 4-day treatments, and the mice were kept in the cage for another 2 weeks with irradiation. Three control groups were  $\gamma$ -irradiated as described but received saline instead of NNK. The whole irradiation period was 31 days, and the total estimated doses were 0.34, 0.68 and 1.02 Gy, respectively. Another control group of mice was treated with NNK as described but without  $\gamma$ -irradiation. The third control was kept in the cage for 31 days without  $\gamma$ -irradiation or NNK treatments. The source of radiation was <sup>137</sup>Cs, and the dose rate was estimated by a fluorescent glass dosimeter. The non-irradiated control groups were placed behind a concrete wall of 1 m thickness. The mice were sacrificed by cervical vertebral dislocation. The liver and lung were removed, placed immediately in liquid nitrogen, and stored at -80 °C until analysis.

### 2.2. DNA isolation and in vitro packaging of DNA

High-molecular-weight genomic DNA was extracted from the lung and the liver using the RecoverEase DNA Isolation Kit (Stratagene, La Jolla, CA). Lambda EG10 phages were rescued using Transpack Packaging Extract (Stratagene, La Jolla, CA).

### 2.3. *gpt* mutation assay

The *gpt* mutagenesis assay was performed according to previously described methods [17]. Briefly, *Escherichia coli*

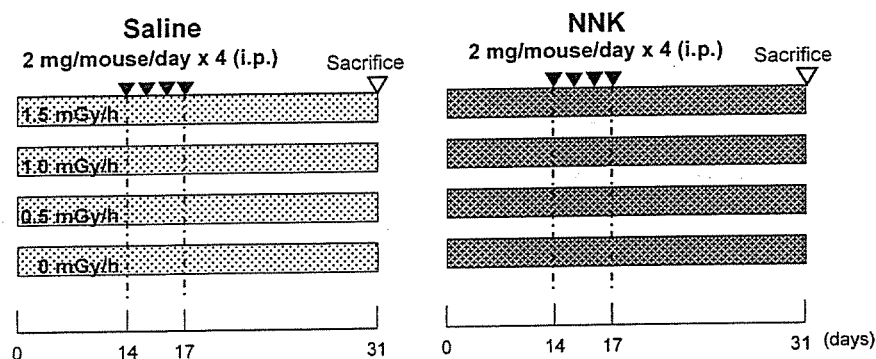


Fig. 1. An experimental design to examine the combined genotoxicity of  $\gamma$ -irradiation and NNK treatments in the lung of mice. Female 7-week-old *gpt* delta mice were divided into eight groups each composed of six mice. Three groups of mice were irradiated at a dose rate of 0.5, 1.0 or 1.5 mGy/h for 22 h/day for 14 days and treated with NNK at a daily dose of 2 mg/mouse for four consecutive days. The irradiation continued during the NNK treatments and the following 14 days before sacrifice. The total radiation doses were 0.34, 0.68 and 1.02 Gy, respectively. Control three groups of mice were  $\gamma$ -irradiated but without NNK treatments. Another control group was treated with NNK but without  $\gamma$ -irradiation. The third control was kept in the cage for 31 days without  $\gamma$ -irradiation or NNK treatments. Transgene  $\lambda$ EG10 DNA was rescued from the lung of mice, and the base substitutions and deletions were analyzed by *gpt* and *Spi*<sup>-</sup> selection, respectively.

YG6020 expressing Cre recombinase was infected with the rescued phage. The bacteria were then spread onto M9 salts plates containing chloramphenicol (Cm) and 6-thioguanine (6-TG), and incubated for 72 h at 37 °C for selection for the colonies harboring a plasmid carrying the Cm acetyltransferase (*cat*) gene and a mutated *gpt* gene. The 6-TG-resistant colonies were streaked again onto the same selection plates for confirmation of the resistant phenotype. All the confirmed *gpt* mutants recovered from the lung were sequenced and the identical mutations from the same mouse counted one mutant. The *gpt* MFs in the lung were calculated by dividing the number of the *gpt* mutants after sequencing by the number of rescued plasmids, which was estimated from the number of colonies on plates containing Cm but without 6-TG. Since no *gpt* mutants recovered from the liver were sequenced, the MFs in the liver were calculated by dividing the number of confirmed 6-TG-resistant colonies by the number of rescued plasmids.

#### 2.4. PCR and DNA sequencing analysis of 6-TG-resistant mutants

A 739 bp DNA fragment containing the *gpt* gene was amplified by polymerase chain reaction (PCR) using primers 1 and 2 [17]. The reaction mixture contained 5 pmol of each primer and 200 mM of each dNTP. PCR amplification was carried out using Ex Taq DNA polymerase (Takara Bio, Shiga, Japan) and performed with a Model PTC-200 Thermal Cycler (MJ Research, Waltham, MA). PCR products were analyzed by agarose gel electrophoresis to determine the amount of the products. DNA sequencing of the *gpt* gene was performed with BigDye™ Terminator Cycle Sequencing Kit (Applied Biosystems, Foster City, CA) using sequencing primer *gptA2* (5'-TCTCGCGCAACCTATTTTCCC-3'). The sequencing reaction products were analyzed on an Applied Biosystems model 310 genetic analyzer (Applied Biosystems, Foster City, CA).

#### 2.5. *Spi*<sup>-</sup> mutation assay

The *Spi*<sup>-</sup> assay was performed as described previously [17]. The lysates of *Spi*<sup>-</sup> mutants were obtained by infection of *E. coli* LE392 with the recovered *Spi*<sup>-</sup> mutants. The lysates were used as templates for PCR analysis to determine the deleted regions. Sequence changes in the *gam* and *redAB* genes, and the outside of the *gam/redAB* genes were identified by DNA sequencing analysis [22]. The appropriate primers for DNA sequencing were selected based on the results of PCR analysis. The entire sequence of  $\lambda$ EG10 is available at <http://dgm2alpha.nhis.go.jp>.

#### 2.6. Statistical analysis

All data are expressed as mean  $\pm$  standard deviations of the MFs of six mice for lung and those of four mice for liver. Differences between groups were tested for statistical significance using a Student's *t*-test. A *p* value less than 0.05 denoted the presence of a statistically significant difference.

### 3. Result

#### 3.1. *gpt* MFs in the lung of NNK-treated and $\gamma$ -irradiated *gpt* delta mice

We measured the *gpt* MFs in the lung of *gpt* delta mice untreated or treated with NNK in the absence or the presence of  $\gamma$ -irradiation (Fig. 2). NNK treatments significantly enhanced the MFs over the control groups. The mean MFs ( $\times 10^{-6}$ ) of NNK-treated versus saline-treated groups were  $14.3 \pm 6.9$  versus  $4.2 \pm 4.0$ ,  $20.7 \pm 5.1$  versus  $4.7 \pm 3.0$ ,  $15.2 \pm 7.3$  versus  $2.0 \pm 2.1$  and  $17.2 \pm 7.9$  versus  $2.7 \pm 1.4$  at the dose rates of 0, 0.5, 1.0 and 1.5 mGy/h, respectively. The  $\gamma$ -irradiation

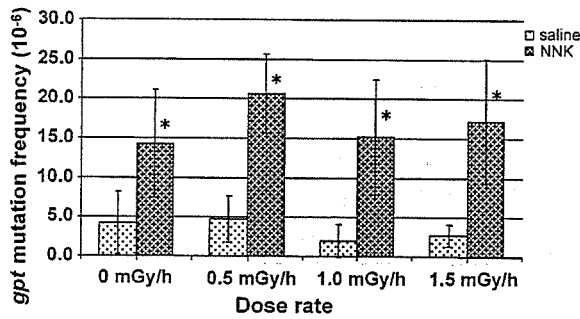


Fig. 2. *gpt* MFs in the lung of mice untreated or treated with NNK in the absence or the presence of  $\gamma$ -irradiation. An asterisk (\*) denotes  $p < 0.05$  ( $n = 6$ ) in a Student's *t*-test of MF of NNK-treated vs. the corresponding untreated mice. Vertical bars show the standard deviations with mice as the unit of comparison.

alone, i.e., the saline-treated group, did not enhance the *gpt* MF under the conditions. Hence, the increases in MFs are due to NNK treatments. Although the individual MFs slightly varied, there was no significant difference among the four MFs of the NNK-treated groups. Thus, we suggested that the irradiation did not modify the genotoxicity of NNK in the lung of mice.

To confirm the results in the lung, we analyzed the *gpt* MFs in the liver of the NNK-treated and saline-treated groups. The mean MFs ( $\times 10^{-6}$ ) of NNK-treated versus saline-treated groups were  $134 \pm 48$  versus  $8.1 \pm 3.8$ ,  $105 \pm 31$  versus  $8.7 \pm 3.5$ ,  $101 \pm 18$  versus  $8.0 \pm 4.2$  and  $128 \pm 76$  versus  $6.8 \pm 0.6$  at the dose rates of 0, 0.5, 1.0 and 1.5 mGy/h, respectively. Although NNK treatments induced mutations much more strongly in the liver than in the lung, there were no significant modulating effects of radiation on the NNK-induced mutations in the liver.

The irradiation might modulate specific types of mutations without affecting the total *gpt* MFs. To exam-

ine the possibility, we determined the mutation spectra of the *gpt* gene in the lung and examined whether the radiation affected specific types of mutations (Table 1). NNK treatments induced G:C to A:T, G:C to T:A, A:T to T:A and A:T to C:G mutations. In particular, A:T to T:A mutations were induced more than 20-fold by NNK treatments. We observed, however, no remarkable variations of mutation spectra associated with the dose rates of combined radiation. Thus, we concluded that the irradiation did not enhance or suppress the base substitutions induced by NNK in the lung of *gpt* delta mice significantly.

### 3.2. *Spi*<sup>-</sup> MFs in the lung of NNK-treated and $\gamma$ -irradiated *gpt* delta mice

Next, we measured the *Spi*<sup>-</sup> MFs in the lung of *gpt* delta mice untreated or treated with NNK in the absence or the presence of  $\gamma$ -irradiation. The mean *Spi*<sup>-</sup> MFs ( $\times 10^{-6}$ ) of NNK-treated versus saline-treated groups were  $5.15 \pm 2.34$  versus  $4.11 \pm 0.98$ ,  $5.47 \pm 1.98$  versus  $5.06 \pm 3.50$ ,  $5.36 \pm 1.56$  versus  $4.09 \pm 0.80$  and  $5.39 \pm 2.56$  versus  $4.65 \pm 1.78$  at the dose rates of 0, 0.5, 1.0 and 1.5 mGy/h, respectively. These results suggest that neither NNK treatments nor the irradiation enhanced the *Spi*<sup>-</sup> MFs in the lung significantly.

To investigate the combined effects of NNK and  $\gamma$ -irradiation on specific types of deletion mutations, we identified all the *Spi*<sup>-</sup> mutations by DNA sequencing analysis (Table 2). Of various classes of deletions observed, only the MFs of large deletions in the size of more 1 kb increased in a dose-dependent manner in the saline-treated group. To examine the dose-response in more detail, we determined the MFs of the large deletions

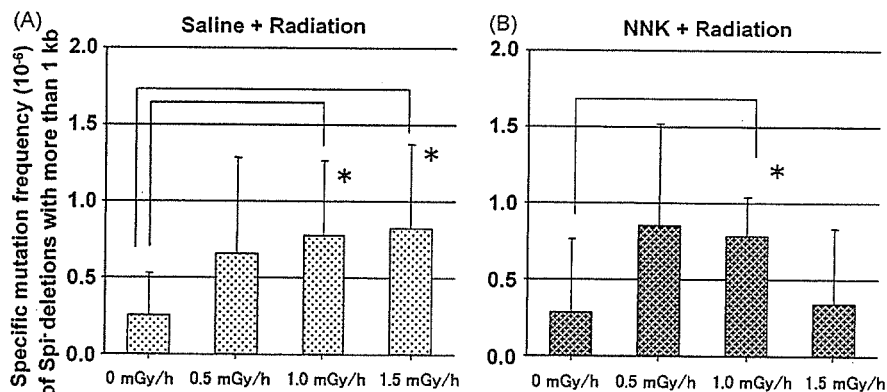


Fig. 3. Specific MF of large deletions with the size of more than 1 kb in the lung of unirradiated or  $\gamma$ -irradiated mice. The mice were not treated (A) or treated with NNK (B). An asterisk (\*) denotes  $p < 0.05$  ( $n = 5$ ) in a Student's *t*-test of MF of  $\gamma$ -irradiated vs. the corresponding unirradiated mice. Vertical bars show the standard deviations with mice as the unit of comparison.

Table 1  
*gprt* mutation spectra in the lung of NNK-treated and  $\gamma$ -irradiated *gprt* delta mice

Treatment: saline	0 mGy/h			0.5 mGy/h			1.0 mGy/h			1.5 mGy/h		
	No.	MF ( $\times 10^{-6}$ )	%	No.	MF ( $\times 10^{-6}$ )	%	No.	MF ( $\times 10^{-6}$ )	%	No.	MF ( $\times 10^{-6}$ )	%
Base substitution												
Transition												
G:C $\rightarrow$ A:T	15(6)	1.81	43	12(6)	1.76	38	5(2)	0.61	29	8(4)	0.81	30
A:T $\rightarrow$ G:C	2	0.24	6	4	0.59	13	1	0.12	6	2	0.20	7
Transversion												
G:C $\rightarrow$ T:A	1	0.12	3	5(2)	0.73	16	1	0.12	6	6(1)	0.61	22
G:C $\rightarrow$ C:G	1	0.12	3	0	0.00	0	0	0.00	0	2(2)	0.20	7
A:T $\rightarrow$ T:A	1	0.12	3	1	0.15	3	1	0.12	6	1	0.10	4
A:T $\rightarrow$ C:G	3	0.36	9	1	0.15	3	1	0.12	6	1	0.10	4
Deletion												
-1 bp	8	0.97	23	6	0.88	19	7	0.85	41	6	0.61	22
>2 bp	3			2			5			3		
Insertion												
	3	0.36	9	3	0.44	9	1	0.12	6	1	0.10	4
Others												
	1	0.12	3	0	0.00	0	0	0.00	0	0	0.00	0
	35	4.23	100	32	4.69	100	17	2.06	100	27	2.73	100
Treatment: NNK												
Base substitution												
Transition												
G:C $\rightarrow$ A:T	24(2)	5.11	36	45(8)	8.02	39	32(5)	5.85	39	54(6)	8.51	50
A:T $\rightarrow$ G:C	0	0.00	0	7	1.25	6	6	1.10	7	2	0.32	2
Transversion												
G:C $\rightarrow$ T:A	9(2)	1.92	13	10(1)	1.78	9	7(1)	1.28	8	7(1)	1.10	6
G:C $\rightarrow$ C:G	0	0.00	0	2	0.36	2	0	0.00	0	3	0.47	3
A:T $\rightarrow$ T:A	13	2.77	19	26	4.64	22	17	3.11	21	17(1)	2.68	16
A:T $\rightarrow$ C:G	15	3.19	22	12	2.14	10	8	1.46	10	12(1)	1.89	11
Deletion												
-1 bp	5	1.06	8	12	2.14	10	9	1.65	11	12	1.89	11
>2 bp	5			6			4			5		
Insertion												
	1	0.21	2	0	0.00	0	4	0.73	5	1	0.16	1
Others												
	0	0.00	0	2	0.36	2	0	0.00	0	1	0.16	1
	67	14.26	100	116	20.68	100	83	15.18	100	109	17.18	100

No. stands for the number of mutations.

of each mouse and calculated the mean MF and standard derivations. The mean MFs ( $\times 10^{-6}$ ) and standard derivations were  $0.25 \pm 0.28$ ,  $0.66 \pm 0.63$ ,  $0.77 \pm 0.49$  and  $0.82 \pm 0.55$  at the dose rates of 0, 0.5, 1.0 and 1.5 mGy/h, respectively (Fig. 3A). The values at 1.0 and 1.5 mGy/h were about three-fold higher than the value at 0 mGy/h, and the differences were statistically

significant ( $p=0.04$ ). In contrast, the dose-response curve of large deletions in NNK-treated group was a bell shaped (Fig. 3B). The mean MFs ( $\times 10^{-6}$ ) and standard derivations of large deletions in the NNK-treated group were  $0.29 \pm 0.47$ ,  $0.85 \pm 0.66$ ,  $0.78 \pm 0.26$  and  $0.35 \pm 0.48$  at the dose rates of 0, 0.5, 1.0 and 1.5 mGy/h, respectively. It should be noted that the

Table 2  
Spi<sup>-</sup> mutation spectra in the lung of NNK-treated and  $\gamma$ -irradiated *gpt* delta mice

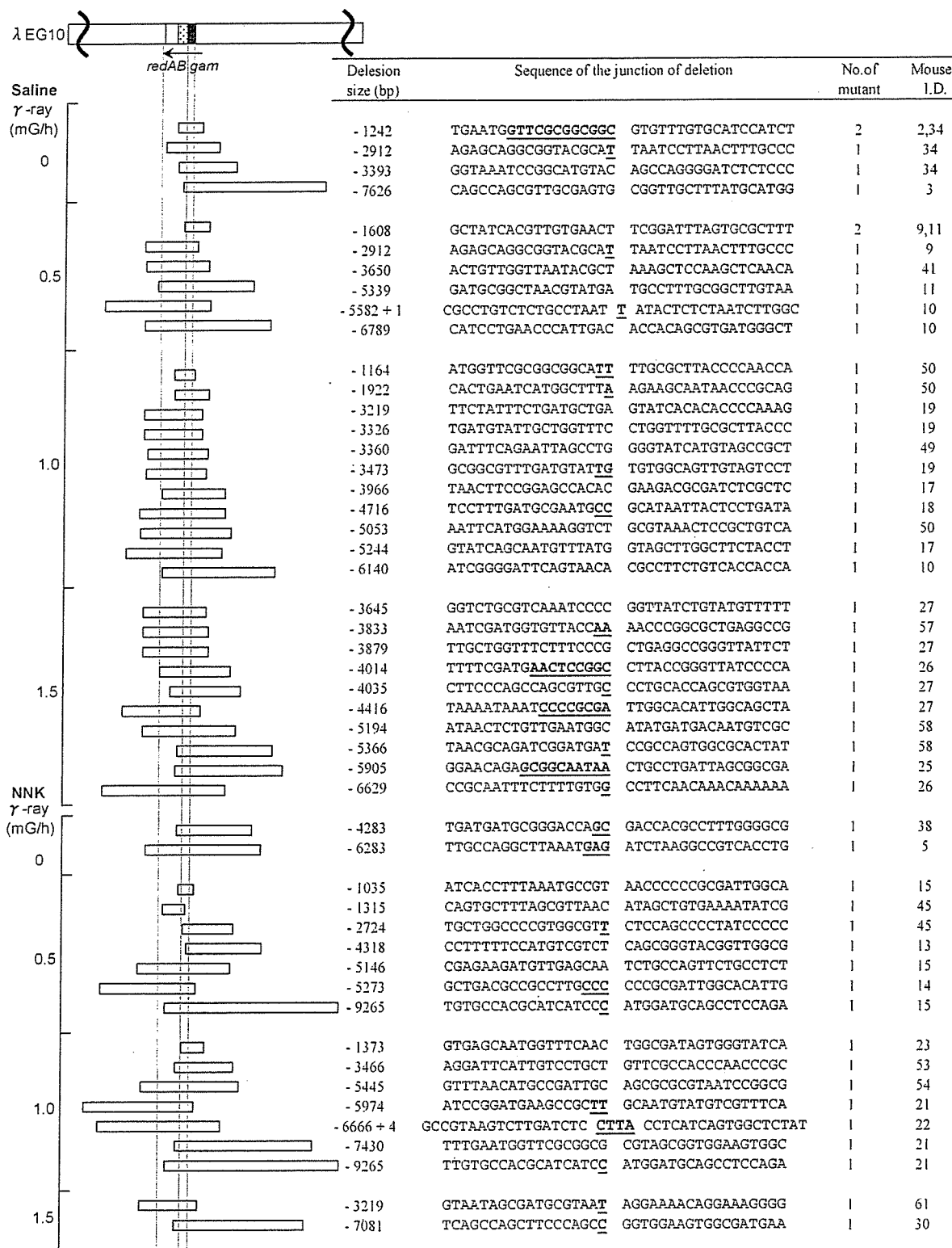
Treatment: saline	0 mGy/h			0.5 mGy/h			1.0 mGy/h			1.5 mGy/h		
	No.	MF ( $\times 10^{-6}$ )	%	No.	MF ( $\times 10^{-6}$ )	%	No.	MF ( $\times 10^{-6}$ )	%	No.	MF ( $\times 10^{-6}$ )	%
<b>1 bp deletion</b>												
<b>Simple</b>												
Guanine	9	0.49	12	7	0.59	12	5	0.34	8	4	0.30	7
Adenine	4	0.22	5	0	0.00	0	2	0.14	3	1	0.08	2
<b>In run</b>												
Guanine	13	0.71	17	15	1.27	25	12	0.82	20	13	0.99	21
Adenine	31	1.70	41	19	1.60	32	22	1.50	37	25	1.91	41
With b.s.	0	0.00	0	0	0.00	0	0	0.00	0	0	0.00	0
<b>&gt;2 bp deletion</b>												
2 bp ~ 1 kb	15	0.82	20	17	1.43	28	17	1.16	28	13	0.99	21
>1 kb	2	0.11	3	7	0.59	12	3	0.20	5	1	0.08	2
>1 kb	5	0.27	7	7	0.59	12	11	0.75	18	10	0.76	16
Complex	8	0.44	11	3	0.25	5	3	0.20	5	2	0.15	3
<b>Insertion</b>												
	3	0.16	4	2	0.17	3	2	0.14	2	5	0.38	8
	75	4.11	100	60	5.06	100	60	4.09	100	61	4.65	100
<b>Treatment: NNK</b>												
	0 mGy/h			0.5 mGy/h			1.0 mGy/h			1.5 mGy/h		
	No.	MF ( $\times 10^{-6}$ )	%	No.	MF ( $\times 10^{-6}$ )	%	No.	MF ( $\times 10^{-6}$ )	%	No.	MF ( $\times 10^{-6}$ )	%
<b>1 bp deletion</b>												
<b>Simple</b>												
Guanine	5	0.61	12	4	0.46	8	4	0.50	9	4	0.48	9
Adenine	3	0.37	7	0	0.00	0	4	0.50	9	1	0.12	2
<b>In run</b>												
Guanine	9	1.10	21	19	2.17	40	9	1.12	21	14	1.68	31
Adenine	12	1.47	29	10	1.14	21	9	1.12	21	15	1.80	33
With b.s.	0	0.00	0	0	0.00	0	2	0.25	5	0	0.00	0
<b>&gt;2 bp deletion</b>												
2 bp ~ 1 kb	12	1.47	29	10	1.14	21	11	1.37	26	11	1.32	24
>1 kb	6	0.74	14	2	0.23	4	3	0.37	7	7	0.84	16
>1 kb	2	0.25	5	7	0.80	15	7	0.87	16	2	0.24	4
Complex	4	0.49	10	1	0.11	2	1	0.12	2	2	0.24	4
<b>Insertion</b>												
	1	0.12	2	5	0.57	10	4	0.50	9	0	0.00	0
	42	5.15	100	48	5.47	100	43	5.36	100	45	5.39	100

No. stands for the number of mutations. Specific MFs of large deletions more than 1 kb in size are italicised.

MF at 1.0 mGy/h ( $0.78 \times 10^{-6}$ ) was about three-fold higher than that of 0 mGy/h ( $p=0.04$ ) but the MF at 1.5 mGy/h ( $0.35 \times 10^{-6}$ ) was very similar to that of 0 mGy/h ( $0.29 \times 10^{-6}$ ). The  $p$  values of the differences

of MFs between saline-treated and NNK-treated groups at dose rates of 0, 0.5, 1.0 and 1.5 mGy/h were 0.44, 0.32, 0.48 and 0.09, respectively. From the results, we suggested that NNK treatments suppressed the induc-

Fig. 4. Molecular nature of large deletions recovered from the lung of *gpt* delta mice untreated or treated with NNK in the absence or the presence of  $\gamma$ -irradiation. Horizontal bars represent the deleted regions of mutants. Most of the mutants lack the entire *gam* gene and part of the *redAB* genes, but some lack the *gam* gene and the upstream region. The *gam* and *redAB* genes make an operon and the transcription starts from the upstream of the *gam* gene. Short homologous sequences in the junctions of the mutants are underlined. Underlined sequences, i.e., T or CTTA, in the middle of two sequences are inserted sequences in the junctions.



tion of large deletions at a dose rate of 1.5 mGy/h of  $\gamma$ -irradiation.

To further characterize the large deletions induced by the irradiation, we identified the size and junctions of all the 51 deletion mutants (Fig. 4). The size of deletions distributed from 1035 to 9265 bp. About half of the mutants had short homologous sequences up to 11 bp in the junctions while another half had no such short homologous sequences. Two mutants had 1 or 4 bp insertions in the junctions. There was no hot spot of the junctions so that only 2 out of 51 deletions were identified in two mice. There were no obvious differences between large deletions induced by radiation alone and those induced by radiation plus NNK treatments. These results suggest that radiation-induced DSBs in DNA caused large deletions either in the absence or the presence of NNK treatments.

#### 4. Discussion

Humans are exposed to a variety of exogenous and endogenous genotoxic agents. Thus, biological effects of radiation at low doses or low-dose-rate should be evaluated in combination with chemical exposure [12]. In fact, survey of chromosome aberrations in habitats in high-background radiation area in China indicates that cigarette smoking has stronger effects on induction of chromosome aberrations than has the elevated level of natural radiation [23]. Epidemiological studies on underground miners exposed to high levels of radon or plutonium suggest the complexity of interactions between radiation and cigarette smoke in induction of lung tumors [24,25]. Hence, it is important to understand the fundamental mechanisms underlying the interactive genotoxicity and carcinogenicity of cigarette smoking and radiation for the risk assessment on human health.

To elucidate the mechanisms involved, we examined the combined genotoxicity of low-dose-rate  $\gamma$ -irradiation and a tobacco-specific nitrosamine NNK in the lung of *gpt* delta mice. In this study, we focused on whether  $\gamma$ -irradiation would modulate NNK-induced base substitutions and whether NNK treatments would modulate radiation-induced deletions. The mice were irradiated at dose rates of 0.5, 1.0 and 1.5 mGy/h for 22 h for 2 weeks and treated with NNK, i.e., 2 mg/mouse/day for four consecutive days, with irradiation (Fig. 1). The mice were irradiated at the same dose rates for another 2 weeks before sacrifice. Base substitutions and deletions in the lung detected by *gpt* and *Spi*<sup>-</sup> selection, respectively, were analyzed at the molecular levels. We chose the dose rates, i.e., 0.5, 1.0 and 1.5 mGy/h of  $\gamma$ -ray,

since Sakai et al. [26] report the suppression of carcinogenicity of 3-methylchloranthrene in ICR female mice by chronic low-dose-rate irradiation of  $\gamma$ -ray at 0.95 mGy/h. According to the report, there is an optimum dose rate of about 1 mGy/h to observe the suppressive effects, and the higher or lower dose rates fail to suppress the tumor induction.

In the present study, NNK treatments significantly enhanced the *gpt* MF (Fig. 2). We observed, however, no modulating effects, i.e., enhancement or suppression, of  $\gamma$ -irradiation at any given dose rate, on the NNK-induced mutations (Fig. 2). This conclusion holds true even when we analyzed the detailed mutation spectra (Table 1). NNK treatments induced similar pattern of base substitutions, i.e., G:C to A:T, G:C to T:A, A:T to T:A and A:T to C:G regardless of the dose rates of combined radiation. In contrast, we observed a suppressive effect of NNK treatments on the radiation-induced deletions.  $\gamma$ -Irradiation enhanced the MF of large deletions in the size of more than 1 kb in a dose-dependent manner (Fig. 3A and Table 2). When combined with NNK treatments, however, the dose–response curve became bell-shaped and the MF at the highest dose rate, i.e., 1.5 mGy/h, was reduced by more than 50% (Fig. 3B and Table 2). The total radiation dose at the highest dose rate was 1.02 Gy. The size of the large deletions was between about 1 and 9 kb, and about half of the large deletions had short homologous sequences in the junctions while other did not (Fig. 4). These features are similar to those of large deletions induced by high dose irradiation with heavy ion, X-ray and  $\gamma$ -ray [20]. Thus, we suggest that NNK induced an adaptive response that eliminated the cells bearing radiation-induced DSBs in DNA.

Previous studies show that low-dose radiation can induce an adaptive response, which causes cells to become resistant to damage by subsequent high doses of radiation [13,27]. Although the exact mechanisms of the adaptive response are not well understood, it is assumed that some proteins are induced by low-dose radiation and they recognize and remove the cells bearing DSB in DNA. Tucker et al. [28] report that the frequency of *Dlb-1* mutations in the small intestine in female F1 mice obtained by crossing SWR/J and C57BL/6 increases along with the total radiation doses of  $\gamma$ -ray, but it saturates and slightly decreases at high doses, i.e., 2–3 Gy (55 mGy/day  $\times$  42 or 63 days). Interestingly, our results also suggest that the MFs of the large deletions saturated slightly at the highest dose of 1.02 Gy (Fig. 3A). Thus the adaptive response might be induced slightly at the highest radiation dose even without NNK treatments. Nevertheless, concomitant NNK treatments much clearly suppressed the occurrence of large dele-



tions at the highest radiation dose. We speculate that NNK treatments plus radiation at the highest dose may induce p53-dependent apoptosis, which eliminates the cells bearing radiation-induced DSBs in DNA [29]. The involvement of p53 in the maintenance of genome stability is associated with several pathways such as cell cycle arrest, apoptosis and DNA repair. Low levels of DNA damage appear to enhance p53-dependent DNA repair while high levels induce apoptosis [30]. We envisage that NNK treatments plus radiation at the highest dose introduce genotoxic damage to the cells, the levels of which are enough to trigger the apoptosis. Zhou et al. [31] examined the combined effects of NNK and  $\alpha$ -particle irradiation with human–hamster hybrid cultured cells and concluded that the induction of chromosome deletions were additive when the NNK dose was low but a suppressive effect was observed at a higher NNK concentration. In vivo studies also suggest that exposure to high levels of cigarette smoke decrease the risk of lung cancer induced by radon in dogs [32]. However, a multiplicative effect of smoking and radon is observed in rats [33]. In humans, the definitive interaction models have not been established between smoking and radiation exposure [24,25]. Thus, further work is needed to clearly establish the interactive genotoxic mechanisms between radiation and cigarette smoking in vivo.

NNK, a tobacco-specific nitrosamine, is metabolically activated by  $\alpha$ -hydroxylation of the methyl and methylene groups [34]. Methylene hydroxylation leads to DNA methylation while methyl hydroxylation leads to pyridyloxobutylated DNA [35]. DNA methylation occurs at N7 and O<sup>6</sup> of guanine and O<sup>4</sup> and O<sup>2</sup> of thymine. It is suggested that O<sup>6</sup>-methylguanine (O<sup>6</sup>-mG) and pyridyloxobutylated DNA are responsible for G:C to A:T and G:C to T:A mutations, respectively, which activate Ki-*ras* oncogene in the mouse lung tumors induced by NNK [6]. In the present study, G:C to A:T and G:C to T:A mutations were induced by NNK treatments significantly (Table 1). Tiano et al. [36] examined the genotoxicity of NNK in AS52 hamster cells expressing human CYP2A6 and analyzed the induced mutations with the *gpt* gene as a reporter gene for mutations. Because of the lack of O<sup>6</sup>-mG methyltransferase in the cell line, about 80% of mutations were G:C to A:T transitions. Interestingly, most of the G:C to A:T transition hotspots occur at the second G of the GGT sequence motif, which is the motif of codon 12 in the Ki-*ras* oncogene [37]. When we define the hotspot as the site where more than four G:C to A:T mutations were identified, we identified 18 hotspots in the *gpt* gene among 155 G:C to A:T mutants recovered from NNK-treated mice. They are nucleotide 27, 64, 86, 87, 92, 107, 110, 113, 115, 116, 128, 274,

281, 287, 402, 409, 417 and 418 when A of ATG of the start codon of the *gpt* gene is set as nucleotide 1. Tiano et al. [36] identified four hotspots of the second G of GGT in nucleotide 23, 116, 128 and 281 in the *gpt* gene, three of which are included in the hotspots identified by us. However, we identified other hotspots such as the second G of GGA at nucleotide 87, 274, 402 and 418, the second G of GGG at nucleotide 27, 64, 92 and 417 and the second G of GGC at nucleotide 113. Thus, we conclude that NNK preferentially induces G:C to A:T mutations at the second G of GGX where X represents any of A, T, G and C. In addition to G:C to A:T and G:C to T:A mutations, we observed an increase in the MFs of A:T to T:A and A:T to C:G in the NNK treated mice (Table 1). Substantial increases in the MFs of A:T to T:A and A:T to C:G are also reported by Hashimoto et al. [38], who examined the genotoxicity of NNK with *lacZ* transgenic mice (Muta<sup>TM</sup> Mouse). Since reporter genes for mutations, such as *gpt*, *cII* or *lacZ*, are not expressed in vivo and are not imposed by any selection bias, they can reflect any genotoxic events occurring in the genomic DNA. In contrast, oncogenes such as the *ras* gene can only detect mutations that can activate the oncogenic activity of the gene products. Thus, we assume that NNK induces modifications in DNA such as O<sup>4</sup>-methyl or O<sup>2</sup>-methyl thymine in the lung, which may account for the induction of A:T to C:G and A:T to T:A mutations, respectively [8]. Although the toxicological significance of these mutations is currently unknown, these mutations may contribute to the carcinogenicity of cigarette smoke as well.

$\gamma$ -Irradiation at dose rate of 1.0 and 1.5 mGy/h clearly enhanced the MFs of large deletions when no NNK treatments were combined (Fig. 3A). The total estimated doses were 0.68 and 1.02 Gy, which may be the lowest radiation doses that gave positive results in transgenic mice mutation assays [16]. In contrast, we could detect no significant increase in the MF of large deletions induced by NNK treatments (Table 2 and Fig. 3A and B). Thus, we suggest that NNK induces mostly base substitutions but not deletions in vivo. Interestingly, NNK treatments induce deletions in cultured mammalian cells. Tiano et al. [36] report that about 20% of mutations induced by NNK treatments are deletions in AS52 hamster cells expressing human CYP2A6. Zhou et al. [31] report that about 80% of NNK-induced mutations are large deletions in the human–hamster hybrid (A<sub>L</sub>) cell assay. We speculate that NNK may have a potential to induce both base substitutions and large deletions in vitro but the latter can be eliminated in vivo by the p53-dependent mechanism. Chinese hamster cell lines such as CHO and V79 harbor missense mutation in the *p53*

gene [39,40]. Large deletions might have been detected in the cultured cells because of inefficient p53 functions.

In summary, we have examined the combined genotoxicity of  $\gamma$ -irradiation and NNK treatments in the lung of *gpt* delta mice. Although radiation did not modulate the NNK-induced base substitutions, NNK treatments suppressed the induction of large deletions in size more than 1 kb induced by the irradiation. NNK treatments might induce an adaptive response, which eliminates the cells bearing radiation-induced DSBs in DNA. This finding may be helpful in understanding the molecular mechanisms of genotoxicity as a result of interactions of more than one genotoxic agents in vivo.

### Acknowledgements

Part of this study was financially supported by the Budget for Nuclear Research of the Ministry of Education, Culture, Sports, Science and Technology, based on the screening and counseling by the Atomic Energy Commission, and the Tutikawa Memorial Fund for Study in Mammalian Mutagenicity.

### References

- [1] R. Doll, R. Peto, The causes of cancer: quantitative estimates of avoidable risks of cancer in the United States today, *J. Natl. Cancer Inst.* 66 (1981) 1191–1308.
- [2] Tobacco smoke and involuntary smoking, IARC Monogr Eval. Carcinog. Risk Chem. Hum., vol. 83, International Agency for Research on Cancer, Lyon, France, 2002.
- [3] S.S. Hecht, Biochemistry, biology, and carcinogenicity of tobacco-specific *N*-nitrosamines, *Chem. Res. Toxicol.* 11 (1998) 559–603.
- [4] S.S. Hecht, Tobacco carcinogens, their biomarkers and tobacco-induced cancer, *Nat. Rev. Cancer* 3 (2003) 733–744.
- [5] International Agency for Research on Cancer Press Release, vol. 154, International Agency for Research on Cancer, Lyon, France, 2004.
- [6] Z.A. Ronai, S. Gradia, L.A. Peterson, S.S. Hecht, G to A transitions and G to T transversions in codon 12 of the *Ki-ras* oncogene isolated from mouse lung tumors induced by 4-(methylnitrosamino)-1-(3-pyridyl)-1-butanone (NNK) and related DNA methylating and pyridyloxobutylating agents, *Carcinogenesis* 14 (1993) 2419–2422.
- [7] R. Guza, M. Rajesh, Q. Fang, A.E. Pegg, N. Tretyakova, Kinetics of *O*<sup>6</sup>-methyl-2'-deoxyguanosine repair by *O*<sup>6</sup>-alkylguanine DNA alkyltransferase within *K-ras* gene-derived DNA sequences, *Chem. Res. Toxicol.* 19 (2006) 531–538.
- [8] E.C. Friedberg, G.C. Walker, W. Siede, R.D. Wood, R.A. Schultz, T. Ellenberger, DNA Repair and Mutagenesis, 2nd ed., ASM Press, Washington, DC, 2006, pp. 1–1118.
- [9] United Nations Scientific Committee on the Effects of Atomic Radiation, Sources, Effects and Risks of Ionising Radiation, 1988 Report to the General Assembly with Annexes, United Nations Press, New York, 1989.
- [10] J.H. Lubin, K. Steindorf, Cigarette use and the estimation of lung cancer attributable to radon in the United States, *Radiat. Res.* 141 (1995) 79–85.
- [11] H.P. Leenhouts, M.J. Brugmans, Calculation of the 1995 lung cancer incidence in The Netherlands and Sweden caused by smoking and radon: risk implications for radon, *Radiat. Environ. Biophys.* 40 (2001) 11–21.
- [12] United Nations Scientific Committee on the Effects of Atomic Radiation, Combined Effects of Radiation and Other Agents, Report to the General Assembly, United Nations Press, New York, 1998.
- [13] M.S. Sasaki, Y. Ejima, A. Tachibana, T. Yamada, K. Ishizaki, T. Shimizu, T. Nomura, DNA damage response pathway in radioadaptive response, *Mutat. Res.* 504 (2002) 101–118.
- [14] T. Lindahl, B. Sedgwick, M. Sekiguchi, Y. Nakabeppu, Regulation and expression of the adaptive response to alkylating agents, *Annu. Rev. Biochem.* 57 (1988) 133–157.
- [15] N.G. Oliveira, M. Neves, A.S. Rodrigues, G.O. Monteiro, T. Chaveca, J. Rueff, Assessment of the adaptive response induced by quercetin using the MNCB peripheral blood human lymphocytes assay, *Mutagenesis* 15 (2000) 77–83.
- [16] T. Nohmi, K.I. Masumura, *gpt* Delta transgenic mouse: a novel approach for molecular dissection of deletion mutations in vivo, *Adv. Biophys.* 38 (2004) 97–121.
- [17] T. Nohmi, T. Suzuki, K. Masumura, Recent advances in the protocols of transgenic mouse mutation assays, *Mutat. Res.* 455 (2000) 191–215.
- [18] M. Miyazaki, H. Yamazaki, H. Takeuchi, K. Saoo, M. Yokohira, K. Masumura, T. Nohmi, Y. Funae, K. Imaida, T. Kamataki, Mechanisms of chemopreventive effects of 8-methoxypsoralen against 4-(methylnitrosamino)-1-(3-pyridyl)-1-butanone-induced mouse lung adenomas, *Carcinogenesis* 26 (2005) 1947–1955.
- [19] T. Nohmi, M. Suzuki, K. Masumura, M. Yamada, K. Matsui, O. Ueda, H. Suzuki, M. Katoh, H. Ikeda, T. Sofuni, Spi<sup>−</sup> selection: an efficient method to detect gamma-ray-induced deletions in transgenic mice, *Environ. Mol. Mutagen.* 34 (1999) 9–15.
- [20] K. Masumura, K. Kuniya, T. Kurobe, M. Fukuoka, F. Yatagai, T. Nohmi, Heavy-ion-induced mutations in the *gpt* delta transgenic mouse: comparison of mutation spectra induced by heavy-ion, X-ray, and gamma-ray radiation, *Environ. Mol. Mutagen.* 40 (2002) 207–215.
- [21] T. Nohmi, K. Masumura, Molecular nature of intrachromosomal deletions and base substitutions induced by environmental mutagens, *Environ. Mol. Mutagen.* 45 (2005) 150–161.
- [22] M. Horiguchi, K.I. Masumura, H. Ikehata, T. Ono, Y. Kanke, T. Nohmi, Molecular nature of ultraviolet B light-induced deletions in the murine epidermis, *Cancer Res.* 61 (2001) 3913–3918.
- [23] W. Zhang, C. Wang, D. Chen, M. Minamihisamatsu, H. Morishima, Y. Yuan, L. Wei, T. Sugahara, I. Hayata, Effect of smoking on chromosomes compared with that of radiation in the residents of a high-background radiation area in China, *J. Radiat. Res. (Tokyo)* 45 (2004) 441–446.
- [24] Z.B. Tokarskaya, B.R. Scott, G.V. Zhuntova, N.D. Okladnikova, Z.D. Belyaeva, V.F. Khokhryakov, H. Schollinger, E.K. Vasilenko, Interaction of radiation and smoking in lung cancer induction among workers at the Mayak nuclear enterprise, *Health Phys.* 83 (2002) 833–846.
- [25] V.E. Archer, Enhancement of lung cancer by cigarette smoking in uranium and other miners, *Carcinog. Compr. Surv.* 8 (1985) 23–37.

- [26] K. Sakai, Y. Hoshi, T. Nomura, T. Oda, T. Iwasaki, K. Fujita, T. Yamada, H. Tanooka, Suppression of carcinogenic processes in mice by chronic low dose rate gamma-irradiation, *Int. J. Low Radiat. I* (2003) 142–146.
- [27] S. Wolff, Failla memorial lecture. Is radiation all bad? The search for adaptation. *Radiat. Res.* 131 (1992) 117–123.
- [28] J.D. Tucker, K.J. Sorensen, C.S. Chu, D.O. Nelson, M.J. Ramsey, C. Urlando, J.A. Heddle, The accumulation of chromosome aberrations and *Dlb-1* mutations in mice with highly fractionated exposure to gamma radiation, *Mutat. Res.* 400 (1998) 321–335.
- [29] C.E. Canman, M.B. Kastan, Role of p53 in apoptosis, *Adv. Pharm.* 41 (1997) 429–460.
- [30] H. Offer, N. Erez, I. Zurer, X. Tang, M. Milyavsky, N. Goldfinger, V. Rotter, The onset of p53-dependent DNA repair or apoptosis is determined by the level of accumulated damaged DNA, *Carcinogenesis* 23 (2002) 1025–1032.
- [31] H. Zhou, L.X. Zhu, K. Li, T.K. Hei, Radon, tobacco-specific nitrosamine and mutagenesis in mammalian cells, *Mutat. Res.* 430 (1999) 145–153.
- [32] F.T. Cross, R.F. Palmer, R.E. Filipy, G.E. Dagle, B.O. Stuart, Carcinogenic effects of radon daughters, uranium ore dust and cigarette smoke in beagle dogs, *Health Phys.* 42 (1982) 33–52.
- [33] F.T. Cross, Radioactivity in cigarette smoke issue, *Health Phys.* 46 (1984) 205–208.
- [34] S.S. Hecht, D. Hoffmann, Tobacco-specific nitrosamines, an important group of carcinogens in tobacco and tobacco smoke, *Carcinogenesis* 9 (1988) 875–884.
- [35] Y. Lao, P.W. Villalta, S.J. Sturla, M. Wang, S.S. Hecht, Quantitation of pyridyloxobutyl DNA adducts of tobacco-specific nitrosamines in rat tissue DNA by high-performance liquid chromatography-electrospray ionization-tandem mass spectrometry, *Chem. Res. Toxicol.* 19 (2006) 674–682.
- [36] H.F. Tian, R.L. Wang, M. Hosokawa, C. Crespi, K.R. Tindall, R. Langenbach, Human CYP2A6 activation of 4-(methylnitrosamino)-1-(3-pyridyl)-1-butanone (NNK): mutational specificity in the *gpt* gene of AS52 cells, *Carcinogenesis* 15 (1994) 2859–2866.
- [37] L.A. Peterson, S.S. Hecht, *O*<sup>6</sup>-Methylguanine is a critical determinant of 4-(methylnitrosamino)-1-(3-pyridyl)-1-butanone tumorigenesis in A/J mouse lung, *Cancer Res.* 51 (1991) 5557–5564.
- [38] K. Hashimoto, K. Ohsawa, M. Kimura, Mutations induced by 4-(methylnitrosamino)-1-(3-pyridyl)-1-butanone (NNK) in the *lacZ* and *cII* genes of Muta Mouse, *Mutat. Res.* 560 (2004) 119–131.
- [39] H. Lee, J.M. Larner, J.L. Hamlin, Cloning and characterization of Chinese hamster p53 cDNA, *Gene* 184 (1997) 177–183.
- [40] W. Chaung, L.J. Mi, R.J. Boorstein, The p53 status of Chinese hamster V79 cells frequently used for studies on DNA damage and DNA repair, *Nucl. Acids Res.* 25 (1997) 992–994.



R00126313\_MUTGEN\_401179